Naval Research Laboratory

Washington, DC 20375-5320

Verification and Validation of Tropospheric Model/Database

JUNHO CHOI
SUNG KWAK
MARA MELTON

Command, Control, Communications, Computers, and Intelligence Branch
Space Systems Development Department

January 19, 1998

DTIC QUALITY INSPECTED 2

19980211 038

REPORT DOCUMENTATION PAGE

Public reporting burden for this collection of information is estimated to average 1 hour per response, including the time for reviewing instructions, searching existing data sources, gathering and maintaining the data needed, and completing and reviewing the collection of information. Send comments regarding this burden estimate or any other aspect of this collection of information, including suggestions for reducing this burden, to Washington Headquarters Services, Directorate for Information Operations and Reports, 1215 Jefferson Davis Highway, Suite 1204, Arlington, VA 22202-4302, and to the Office of Management and Budget. Paperwork Reduction Project (0704-0188), Washington, DC 20503.

1. AGENCY USE ONLY (Leave Blank)	2. REPORT DATE January 19, 1998	3. REPORT TYPE AND DATES COVERED

4. TITLE AND SUBTITLE

Verification and Validation of Tropospheric Model/Database

5. FUNDING NUMBERS

6. AUTHOR(S)

Junho Choi, Sung Kwak, and Mara Melton

7. PERFORMING ORGANIZATION NAME(S) AND ADDRESS(ES)

Naval Research Laboratory
Washington, DC 20375-5320

8. PERFORMING ORGANIZATION REPORT NUMBER

NRL/MR/8140--98-8130

9. SPONSORING/MONITORING AGENCY NAME(S) AND ADDRESS(ES)

10. SPONSORING/MONITORING AGENCY REPORT NUMBER

11. SUPPLEMENTARY NOTES

12a. DISTRIBUTION/AVAILABILITY STATEMENT

Approved for public release; distribution unlimited.

12b. DISTRIBUTION CODE

13. ABSTRACT (Maximum 200 words)

A verification and validation of tropospheric models and databases has been performed based on ray-tracing algorithm, statistical analysis, test on real-time system operation, and other technical evaluation process. Databases are examined for pressure levels, adequate humidity, and temperature representation with respect to each layer and location. Anay missing grid point and wrong data hase been corrected or inserted through a linear interpolation process. Three models are verified through 130 areas of interest in order to avoid any complexity and time. Model performances are examined for time-delay, standard deviation, angle of arrival and azimuch sensitivity. Modified exponential model outperforms othe models and ECM or HIRAS data are more realistic in applying to the operating system.

14. SUBJECT TERMS

Troposphere	HIRAS	MRF	FNL	Modified exponential model
Hopfield	Ray trace	Geodetic	ECEF	Range error
ECM	Angle of arrival error	Time delay		

15. NUMBER OF PAGES 69

16. PRICE CODE

17. SECURITY CLASSIFICATION OF REPORT	18. SECURITY CLASSIFICATION OF THIS PAGE	19. SECURITY CLASSIFICATION OF ABSTRACT	20. LIMITATION OF ABSTRACT
UNCLASSIFIED	UNCLASSIFIED	UNCLASSIFIED	UL

NSN 7540-01-280-5500

CONTENTS

VERIFICATION AND VALIDATION OF TROPOSPHERIC MODEL/DATABASE

1. INTRODUCTION

The study of the effects of the atmosphere on microwave propagation necessitates a knowledge of height variation of refractive index in tropospheric and ionospheric regions. Since the magnitude of the refractive index is a function of such parameters as geographic location, weather, time of the day, and season of the year, it becomes an overwhelming task to analyze atmospheric propagation effects under parametric conditions. The troposphere research team has developed an atmospheric model, in which representatives of average climatology(ECMWF and HIRAS) data and meteorology(MRF and FNL) data are employed, for system engineers or researchers in microwave and optical wave propagation field. Since the system engineer in the propagation field needs a few propagation parameter values for system design, the researcher must develop the propagation models either to verify the model or to generate a new model.

This document summarizes the verification and validation techniques applied to databases and models developed under the Tropospheric Research Project at the Naval Research Laboratory. During the course of this project, several climatological data sets are processed and evaluated by using the ray trace algorithm and statistical data analysis. Two data formats are derived for each data source. The first data format is the multilayer 17-variable data. The second data format, 7-variable surface data, is derived from the multilayer data. Using the 7-variable surface information, the Modified Exponential Model[1,2] builds a multilayer atmosphere. The constructed atmospheric data is then used with Millman's Stratified Layer Method[3] to calculate range error, time delay, and angle of arrival error. In addition to the surface climatology data, error parameter statistics are delivered under this project. Specifically, worldwide time delay and angle of arrival error standard deviations are provided. In addition, these error standard deviations are sensitive to azimuth variation.

This paper describes the methods, algorithms and safeguards used in verifying and validating modified tropospheric models with climatology databases such as ECMWF and HIRAS. This tropospheric model code may be easily interfaced with other users. There are two data files for modified tropospheric model such as meteorological and reference height data. These two data files should generate more accurate time delay, range error, and angle of arrival error because these data files consist of meteorological data and reference coefficient height for each grid rather than an average constant. Also, this modified tropospheric model can be accessible to real time weather data.

2. DATABASE VERIFICATION

2.1 Data Sources

Climatological data are obtained from numerous sources including the Air Force, the Navy and the NOAA. Surface data from the following four databases is derived.

2.1.1. European Center for Medium Range Weather Forecast (ECMWF)

ECMWF data was obtained from the US Air Force Environmental Technical Applications Center (ETAC) at Scott Air Force Base, Illinois. The data consists of averaged monthly over the years 1981-1991 with 2.5 x 2.5 degree grids. There are 14 layers of data by geopotential height and pressure levels from 20 to 1000 millibars (mbars). The data elements include latitude, longitude, temperature, dew point, air density, and number of observations used to obtain mean and standard deviation values.

2.1.2 High Resolution Analysis System (HIRAS)

HIRAS data was obtained from the ETAC, Scott Air Force Base, Illinois. The data includes monthly and 6-hourly averaged climatology data over a nine-year period with 2.5 x 2.5 degree grids around the world. There are 14 layers data by geopotential height and pre-defined pressure levels from 10 to 1000 mbars. Other data elements include temperature, relative humidity, latitude, longitude, date, and time. Associated heights from the ECMWF data are used with the HIRAS data upon full consultations with engineer and scientists who generated the data.

2.1.3 Medium Range Forecast (MRF)

MRF data from the NCDC, NOAA, includes 6 hourly diurnal meteorological data over the period of 1st January 1991 to 31st December 1996, with 2.5 x 2.5 degree grids around the world. There are 12-layers from the surface to the height of 50 mbars. The data elements include geopotential height, air temperature, relative humidity, wind vector and speed, latitude, longitude, date, and time.

2.1.4 Final Analysis (FNL)

FNL Data are the version of the improved MRF Data consisting of 6 hourly diurnal meteorological data over the period of 1st January 1997 to present with 1.0 x 1.0 degree resolution around the world. There are 13 layers from the Earth's surface to the height of 20 mbars. Data elements include geopotential height, temperature, relative humidity, total cloud cover, wind vector and speed, geopotential height and pressure vertical velocity.

2.2 Processing Multilayer Data

ECMWF data are delivered in unformatted ASCII text. HIRAS data are delivered in formatted ASCII text. MRF and FNL are converted into ASCII data from binary. All four data sources are converted into the troposphere global 17-variable multilayer format. See appendix A for a description of the troposphere database format. ECMWF, HIRAS, and MRF data sets were defined for each of 2.5° x 2.5° grids; 10,368 total. FNL dataset is the improved MRF data. The resolution of FNL data are 1° x 1° resolution as opposed to the 2.5° x 2.5° resolution of the other data sources. These data are checked to ensure valid ranges. Minimum and maximum field values are calculated and checked for reasonableness.

Occasionally, a missing value is appeared in the raw data for a parameter such as relative humidity. Missing data are indicated consistently by a zero value where a zero value was unreasonable. For instance, the Table 1 presents a sample dataset with a zero relative humidity value at 850 mbars pressure level. It is expected that relative humidity would decrease with increasing height and with decreasing pressure. A linear fit using the two nearest temperatures and pressures would be used to interpolate the relative humidity at the 850 mbars pressure level and the surface pressure level.

Table 1. Sample Data Anomaly for ECMWF, HIRAS and MRF

Pressure (mbars)	Temperature (°k)	Relative Humidity (%)	Geopotential Height (m)
20	221	0	26354
30	216	0	23734
50	207	0	20603
70	199	0	18624
100	198	0	16565
150	206	0	14181
200	218	0	12387
250	230	0	10918
300	239	37.6	9666
400	255	42.8	7577
500	267	47.3	5870
700	282	52.6	3160
850	293	0	1520
1000	301	63.4	104

Although pressure layer data are not expected to be strictly increasing or decreasing, all 10,368 grids data are read and anomalous records written to a file for review and assessment. Abnormal data in temperature and height are considered to be strictly

3

increasing/decreasing. Anomalous relative humidities are out of range and negative height or "zero" data are not reasonable for each level. Each of the anomalous records is reviewed and corrected through interpolation process. If the value was determined to be missing, a simple linear interpolation corrects the missing value. MRF and FNL data sets are in polar coordinates. In order to assign our coordinates, grid system is used to unpack and convert the binary data. Additional code has been developed to use linear interpolation to fill the missing grids that are resulted from polar-to-cartesian coordinate conversion.

2.3 Validation and Verification of Multilayer Data

The 17 variable multilayer data are contain several occurrences of negative height at 1000 mbars pressure level. This is due to the fact that surface pressure is less than 1000 mbars at certain points. In order to use the data for raytracing, pressure is interpolated for zero height where a negative height occurred. In addition, data are checked for zero temperature and zero relative humidity for 700 mbars, 800 mbars, and 1000 mbars and interpolated these values whenever necessary. The program then calculates refractivity and dry/wet heights for the new readings. As a final effort, the global database is checked to ensure that 14 multilayers occurred for each reported grid and no negative heights, zero temperatures or zero relative humidities occurred above 400 mbars. Worldwide contour maps are plotted for pressure, refractivity, temperature and relative humidity for different data sources and visually inspected for patterns as well as reasonableness. Figure 1a and 1b show worldwide contour maps for ECMWF and MRF data source of refractivity.

2.4. Surface and Reference Coefficient Data

The processed 17 variable multilayer data need lots of memory for storage. ECMWF data need about 6 Mbytes for uncompressed data. HIRAS data need 4 times more than ECMWF data about 24 Mbytes for uncompressed data. MRF data need about 730 Mbytes for one year uncompressed data. FNL data need about 1.2 Gbytes for one month uncompressed data. It is inappropriate to use the processed 17 variable multilayer data. Therefore the seven variable surface data is generated from the 17 variable multilayer data. Surface data is defined as data where height equals zero. Surface data is provided. The data is a result of setting height equal to zero and interpolating the remaining elements. The interpolation process uses a second order polynomial fit which seems to produce the closest approximation to the multilayer data. The surface database is organized in a series of 2.5° x 2.5° grids. The grids are numbered beginning with grid number 1 at 0 degree latitude and 0 degree longitude(Greenwich, England) and subsequent grids follow the equator in an easterly direction from 0 degree longitude to 357.5 degree longitude. The second row begins at 2.5 degree latitude and 0 degree longitude and encircles the earth in an easterly direction. This continues to 87.5 degree latitude and 357.5 degree longitude for northern hemisphere. There is no data for the ring at exactly 90 degree north. The next series of grids begin at -2.5 degree latitude and 0 degree longitude and terminate at -90.0 degree latitude and 357.5 longitude for the southern hemisphere. Figure 2 shows the database organization of each data (ECMWF,

4

Figure 1a- ECMWF Multilayer Refractivity(N) at 1000mb Contour Map for August, 10 year average
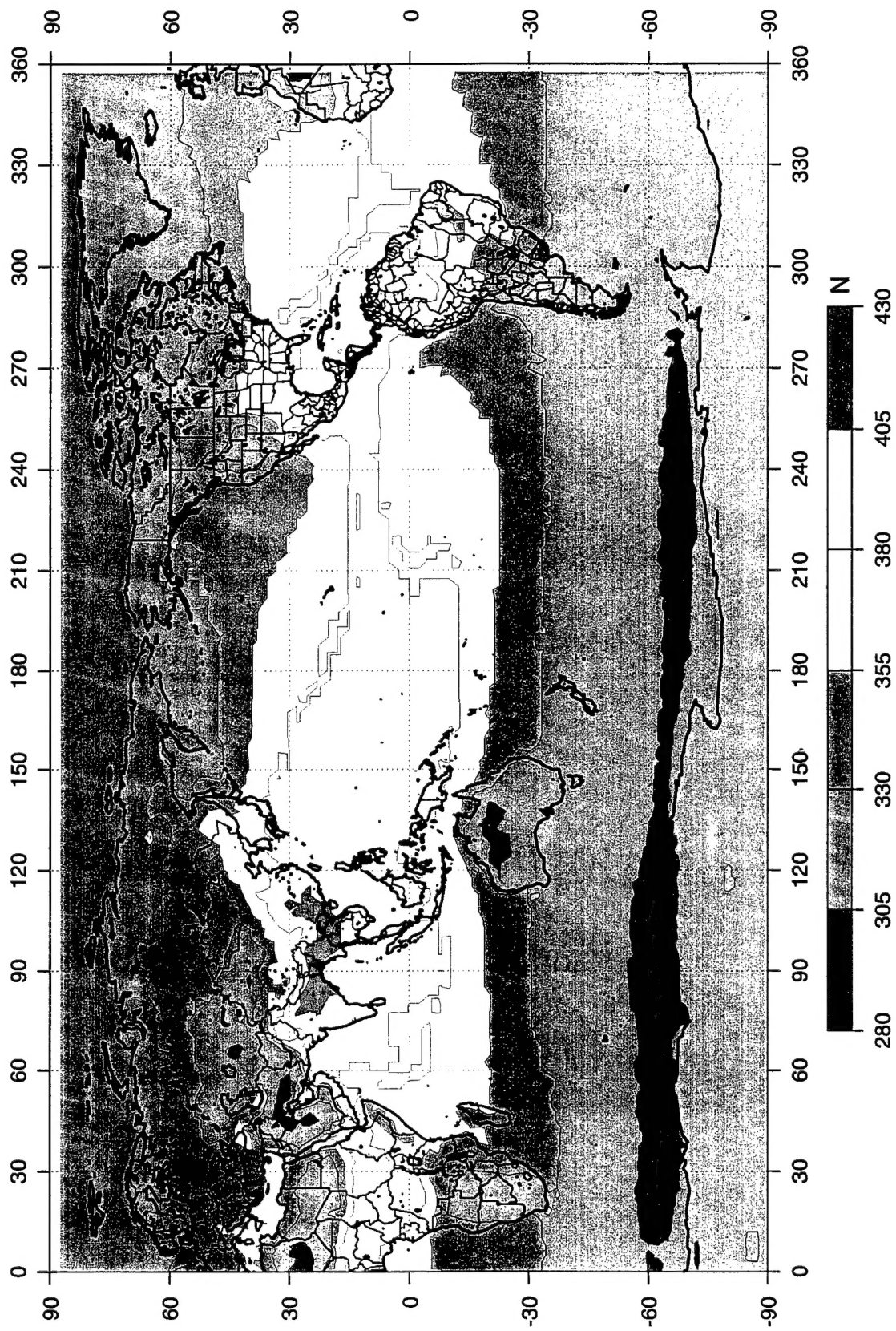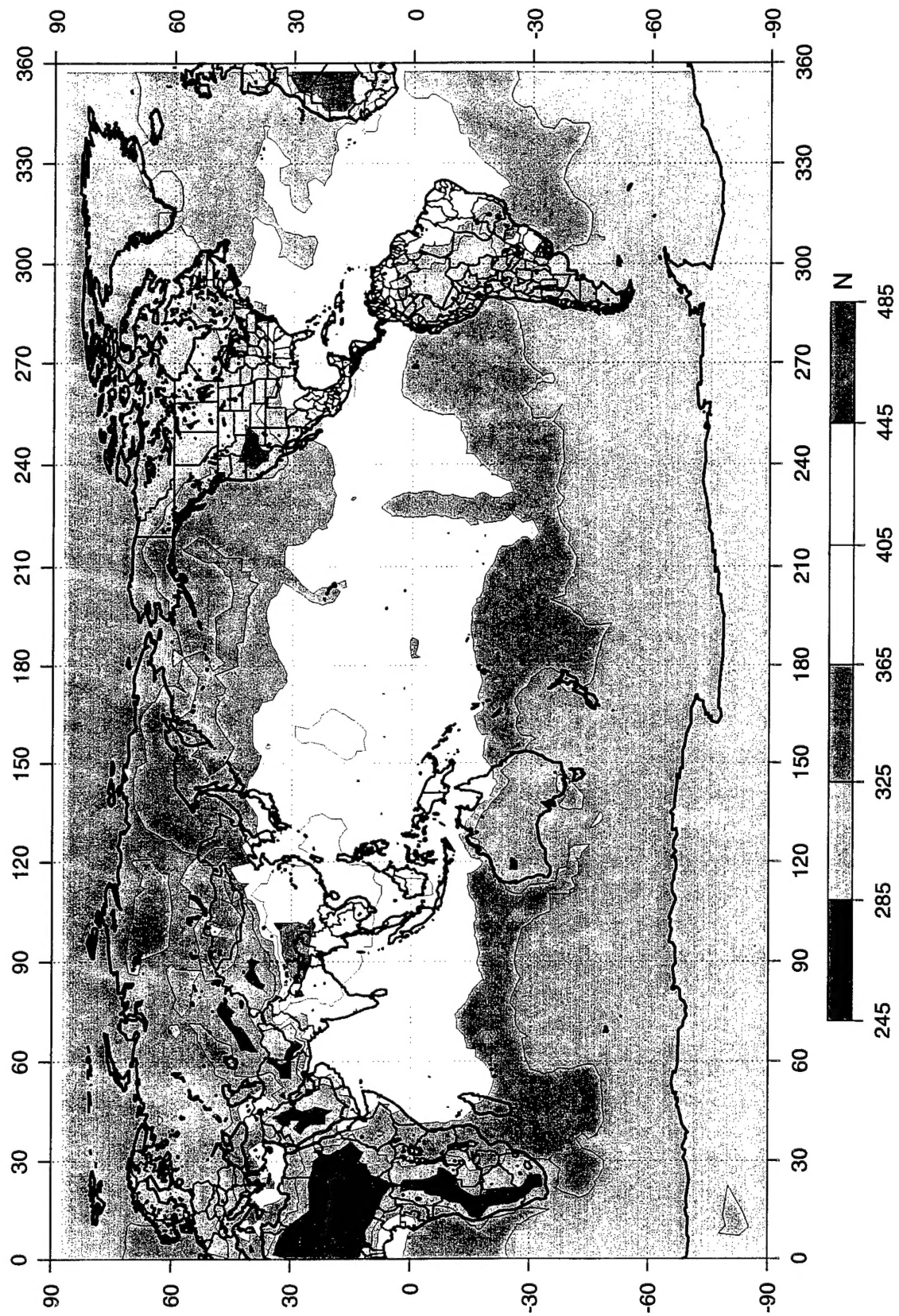
Figure 1b- MRF Multilayer Refractivity(N) at 1000mb Contour Map for August 9 at 1800
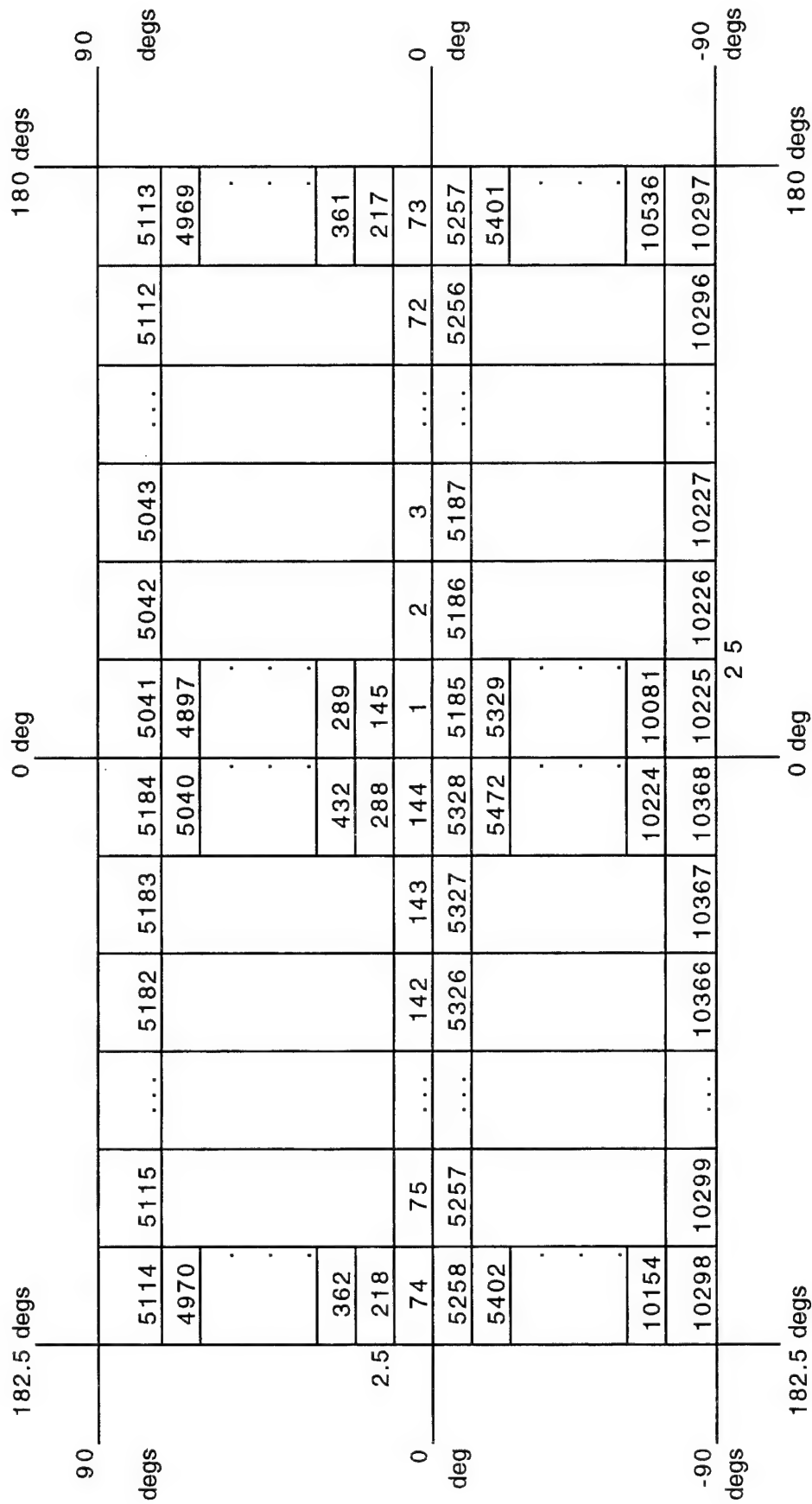
N

245   285   325   365   405   445   485

Figure 2 Database organization for global map

HIRAS, and MRF). For example, the grid number 1 contains areas that are covered in the area of greater than or equal to 0 degree latitude and less than 2.5 degree latitude and are covered in the area greater than or equal to 0 degree longitude and less than 2.5 degree longitude. The grid number 2 continues areas that are covered in the area of greater than or equal to 0 degree latitude and less than 2.5 degree latitude and all longitudes that are greater than or equal to 2.5 degree longitude and less than 5.0 degree longitude. This logic is followed for the remaining grids. Table 2 contains a sample of surface data. Pressure (Press), refractivity (N), temperature (T), and relative humidity (RH) are interpolated for each day/time period for each of the four data sources. Figure 3 through 5 show surface refractivity contour maps for ECMWF, HIRAS, and MRF dataset.

Table 2. Surface Data format for each data file (ECMWF, HIRAS, MRF, and FNL)

GRID NUMBER	1 through 10,368 Note: latitude 90 deg is not report.
LATITUDE (degree)	Latitude in positive degrees for North, negative degrees for South
LONGITUDE (degree)	Longitude in degrees East, 0 to 360 degree
SURFACE PRESSURE (mbars)	Pressure in millibars
SURFACE REFRACTIVITY (N)	Mean total Refractivity in N units (Ndry + Newt)
SURFACE TEMPERATURE (K)	Mean Temperature in Kelvins
SURFACE RELATIVE HUMIDITY (%)	Mean percentage relative humidity

After the surface data is used in the Modified Exponential Model to build a local atmosphere, Millman's Stratified Layer method of raytracing uses the constructed data to produce the error parameters of interest such as range error, time delay and angle of arrival error.

The reference height coefficient data consists of hourly/daily/monthly/ height coefficients, undulation value, time ,range, and angle of arrival error standard deviation of the tropospheric propagation model for each grid. These coefficients are used to build the tropospheric refractivity to about 20 mbars pressure level from the surface data.   The undulation of geoid is a   distance between the geoid and the mathematical reference ellipsoid as measured along the ellipsoidal normal. This distance is considered positive outside, or negative inside, the reference ellipsoid. Table 3 shows the reference coefficient to each month.

Figure 3- ECMWF Surface Refractivity(N) Contour Map for August, 10 year average
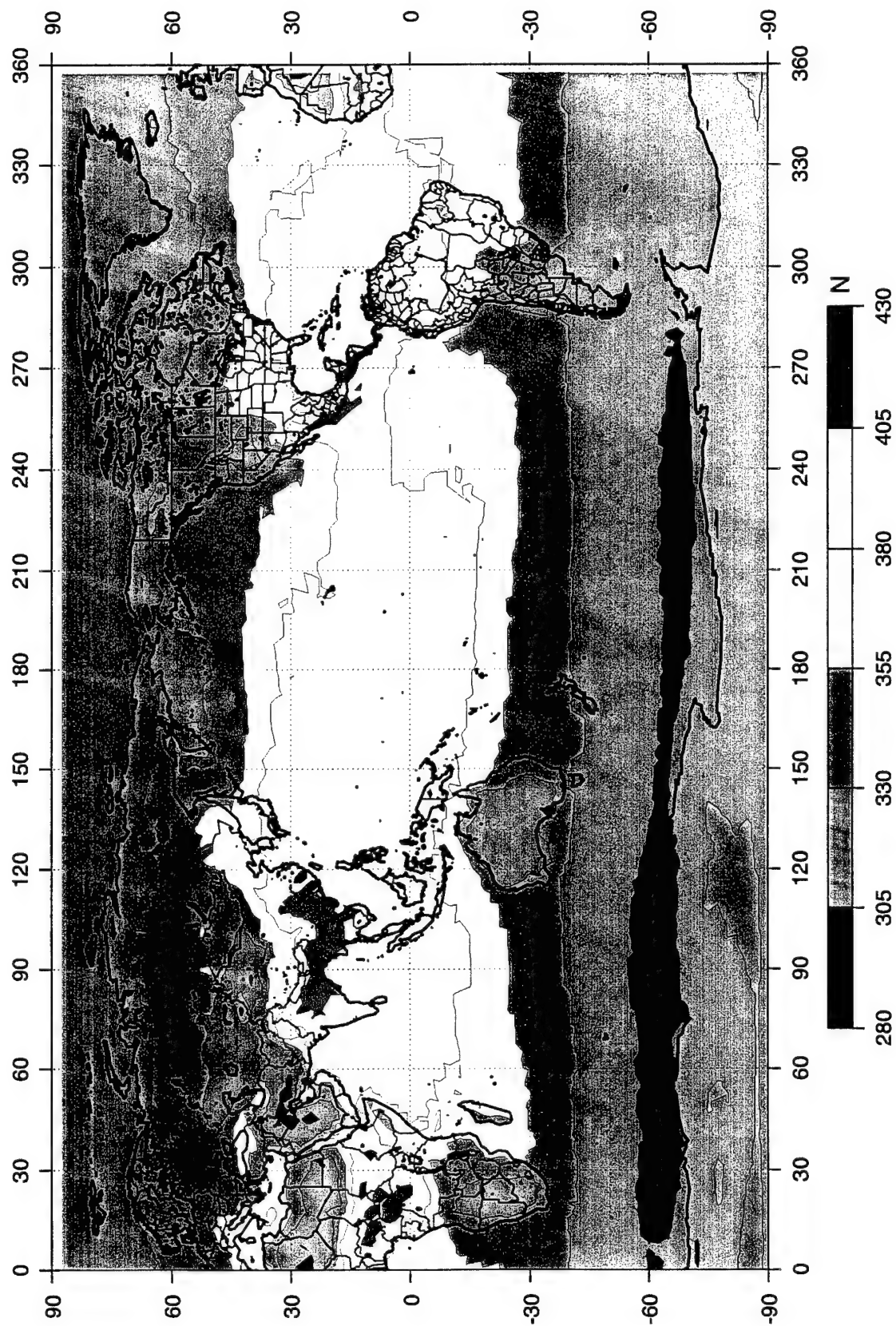
Figure 4- MRF Surface Refractivity(N) Contour Map for August 15 at 0600

N

485 445 405 365 325 285 245
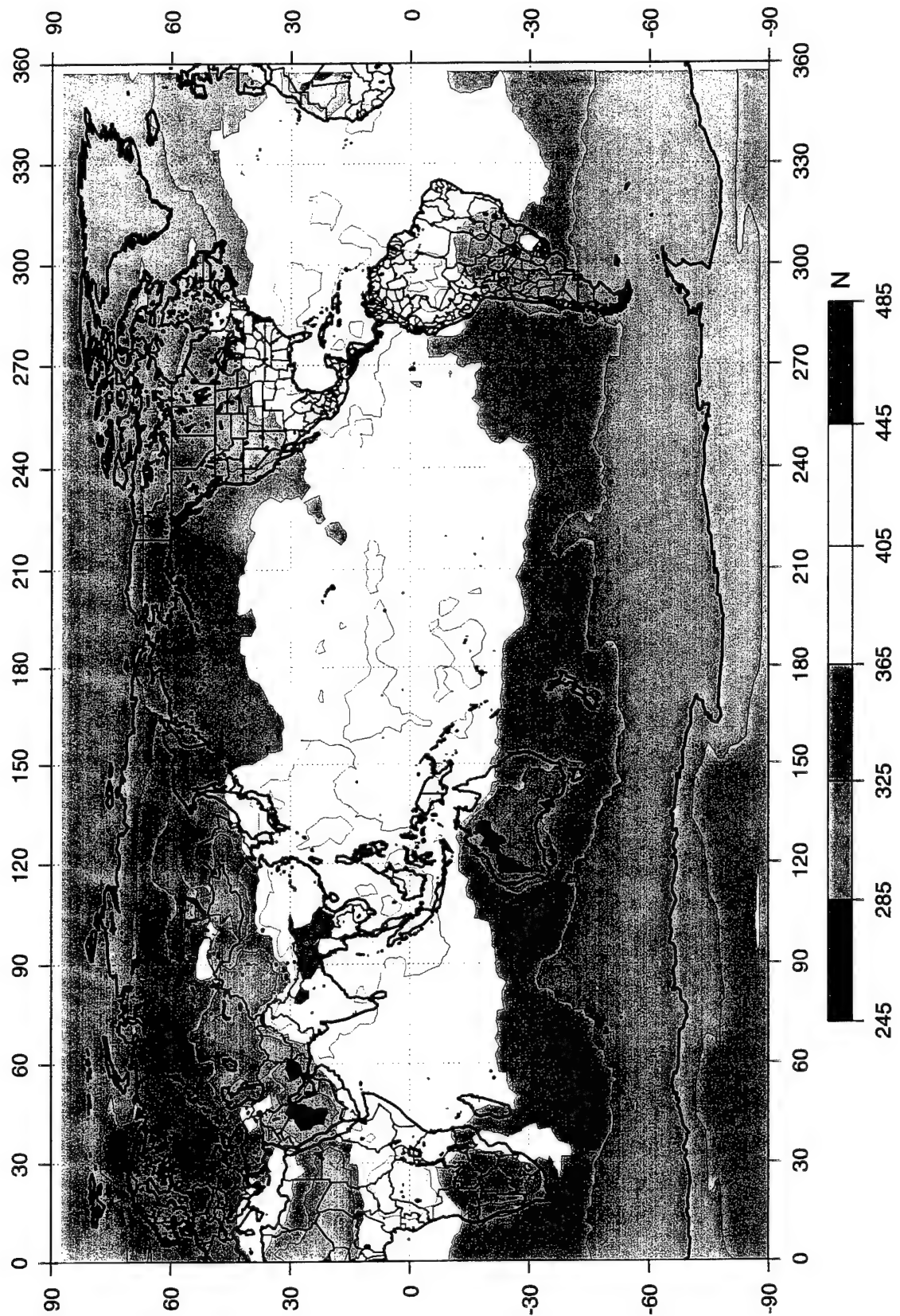
Figure 5- HIRAS Surface Refractivity(N) Contour Map for August at 0600
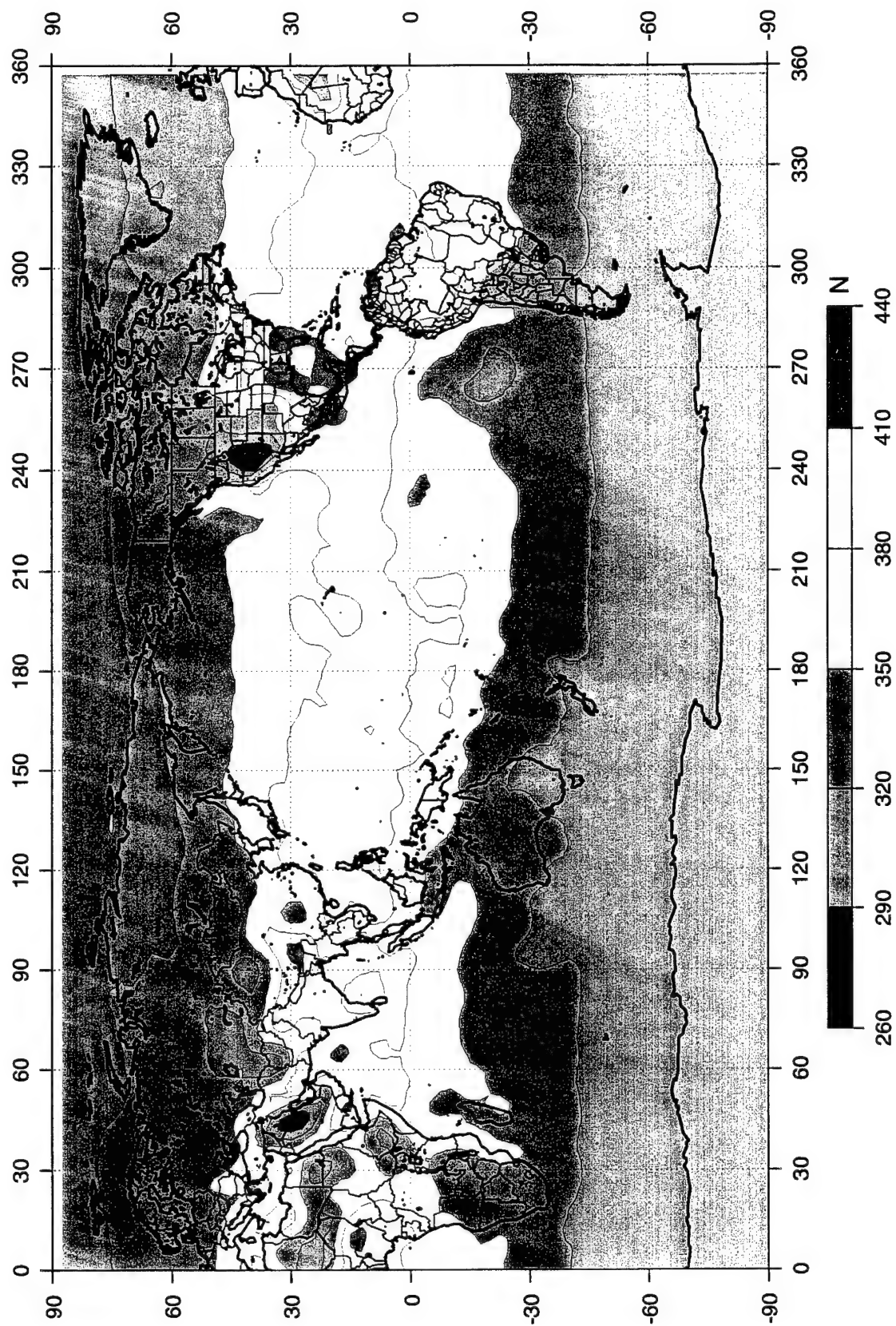
Table 3. The format of reference coefficient datable

# of Grid	Month	Undulation	Standard Deviation Time/Range Error	Standard Deviation Angle Error
1	99.99 Km	± 20.0 m	3.03	0.23
. . .	. . .	. . .	. . .	. . .
10,368	89.00 km	± 13.6 m	4.32	0.06

3. MODEL VERIFICATION

3.1 Verification Strategy

Millman's Stratified Layer method of raytracing divides the troposphere into discrete layers of refractivity n_i. The assigned value may come from actual meteorological measurements (our multilayer data) or from modeled atmospheres. Three models are delivered under this project. The Modified Exponential, Hopfield[4,5], and ESS Models[6,7] are compared with computed error parameters and actual measured multilayer data. Error parameters of interest are time delay, range error and angle of arrival error. Several areas-of-interest (AOIs) were selected to examine the performance results of each model. Approximately 130 AOIs were selected for unique geographic and climatic conditions.

3.2. Modified Exponential Model

Visual inspection of the multilayer data indicates that refractivity is a decreasing exponential function of height. In fact any local refractivity N(h) can be expressed as

$$N (h) = N_s \exp (-h/H)$$

where H is a scale (or reference) height appropriate to the value of N at zero height, N_s. Considering a scale height here, it is simply the height at which the value of N (h) is 1/e of the surface refractivity N_s from the above equation, at which the height h is equal to the scale height H. The wet refractivity, N_w, is below 1.0 N-unit in comparison with the dry refractivity N_d with 100 N-unit in the neighborhood of the selected value of a reference height, H. The ratio of dry to wet refractivity is approximately 100 at the reference height H where the height from the surface is 1/3 of the total tropospheric region. The refractive effect of bending and time delay beyond this layer (reference height) will be very limited

12

since temperature and humidity does not change drastically to affect refractive bending in those extended areas such as tropopause, stratosphere, stratopause, free space and ionosphere above 1 GHz. This coincides with the fact that the most bending and refractive phenomena occur within this region (beneath the reference height) from the surface of the Earth. This implies that the tropospheric effects on the ray bending can be approximated with the reference height without loss of any significant physical principle.

In an inversion layer temperature increases with altitude, and such a layer is highly stable. All vertical motions are strongly inhibited in an inversion layer, and pollution emitted below the layer tends to be confined below it. Also, if a source of water vapor exists below an inversion layer, it tends to be confined below the layer, with the result that large decreases in index of refraction may be encountered in the upward passage through an inversion layer. Thus, the occurrence of inversion layers has an important effect on earth-space communication paths in the low elevation angle. The decrease or change of the water vapor pressure(e) with height is generally variable but may be approximately exponential. Note also that the delay caused by water vapor is considerably smaller than that for dry air above 3 km to 5 km from the surface, but total water vapor content along a path is variable and not predictable with high accuracy from the surface water vapor pressure or density. Therefore, water vapor is responsible for a larger error or uncertainty in the range calculation than in dry air at lower atmosphere. This kind of exponential model is widely applicable and is reliable when any reliable climatological or meteorological data on actual refractivity profiles are applied. In this report a global 2.5^0 x 2.5^0 grid accuracy is used. This model provides the accuracy of less than 1% of root-mean square error (rms) from the climatology or meteorology data in comparison with the accuracy of 20 % to 30 % of rms errors for the Hopfield model and other models. Therefore, this model approach has been chosen in this study as the most reliable and accurate model in comparison with other models for various different conditions.

3.3. Hopfield Model

The actual atmosphere is not isothermal, nor is its composition an ideal gas, and the state of water vapor in the atmosphere is quite different from the state of an ideal gas. So it is more practical to express the refractivity in the quadratic term induced by the dry air or the water vapor separately as follows:

$$N (h) = N_d + N_w$$

where N_d is the dry refractivity and N_w the wet refractivity represented by

$$N_d = k_d (h_{0d} - h)^4$$

$$N_w = k_w (h_{0w} - h)^4$$

with $k_d = 1/[h_{0d} - h_s]^4$, $k_w = 1/[h_{0w} - h_s]^4$, h_{0d} the dry height of the order of 40 km, and h_{0w} the wet height of the order of 12 km. The h_s is the surface height and h is the height

of each layer. It is noted that if the refractivity as a function of height is represented by an exponential, it is not integrable in closed form, where if it has the form as in dry and wet refractivity equations , it is integrable. The representation of the dry and wet terms of refractivity by quadratic equations as dry and wet refractivity equations give a good agreement with range error and Doppler data above 6^0 elevation angles. Note here that if monthly or weekly averages of the refractivity are used and the accuracy is not so important, this model is useful and practical.

3.4. ESS Model

The ESS Model is a second order polynomial equation with varying zenith angle (za) from ground station to satellite. Negative angles are converted to 0 degree and below the horizon measurements (> 90 degrees) are converted to 90 degrees. The equation for a range delay is:

$$RANGEDEL = \frac{D}{A + B*\cos(za) + C * \cos^2 (za)}$$

where   D is equal to 0.3048006.

A = 0.003589	B = 0.087605	C = 0.19696793	$za \leq 5^{\circ}$
A = 0.002129	B = 0.12158	C = 0	$5^{\circ} < za < 30^{\circ}$
A = 0.030000	B = 0.080000	C = 0	$za \leq 30^{\circ}$

4. MODEL VALIDATION

4.1. Selected Area-of-Interest

Raytrace error parameters are dependent on the time and the place. The 130 area-of -interest are selected as the representative geographic and climatic global conditions for the completion of model effectiveness. Table 4 contains a list of these areas of interest with climatic and topographic descriptions. Figures 6 and 7 show time delay and angle error calculated with the Modified Exponential, Hopfield and ESS models using surface data plotted against the actual ECMWF data on August and February data at Tehran, Iran. The results show that the Modified Exponential Model is closest to the measured data, and has been consistent regardless of area-of-interest, month, or data source.

14

Table 4 . Selected Areas-of-Interest

#	AOI	Description	LO LAT	HI LAT	LO LON	HI LON	Hgt MSL	Continent	Climate
1	EUS	Eastern US	22.5	55.0	260.0	300.0		N. America	TEMPERATE
2	WUS	Western US	22.5	55.0	225.0	260.0		N. America	TEMPERATE
3	NEUS	Northeast US	40.0	50.0	285.0	300.0		N. America	TEMPERATE
4	MWUS	Midwest US	30.0	45.0	245.0	260.0		N. America	TEMPERATE
5	AK	Bering Sea	45.0	60.0	165.0	190.0		WATER/Pac	BOREAL
6	SEUS3	Southeast US Region 3	8.0	32.5	275.0	285.0		N. America	SUBTROPICAL
7	EUR	Europe	35.0	70.0	345.0	45.0		Europe	TEMPERATE
8	PG	Persian Gulf	10.0	45.0	30.0	70.0		WATER/Med	TROPICAL
9	MED	Mediterranean	27.5	50.0	345.0	45.0		WATER/Med	TEMPERATE
10	MIO	Mid-Indian Ocean	-15.0	5.0	60.0	90.0		WATER/Mio	TROPICAL
11	FE	East China Sea & Sea of Japan	22.5	50.0	115.0	155.0		WATER/Pac	TEMPERATE
12	NWP	Northwest Pacific	5.0	22.5	135.0	155.0		N. America	TROPICAL
13	CAN	Canada Belt	47.5	60.0	230.0	310.0		N. America	BOREAL
14	CAM	Central America	7.5	22.5	260.0	290.0		N. America	TROPICAL
15	AMFOR	Amazon Forest	-15.0	10.0	285.0	325.0		S. America	TROPICAL
16	SAF	South Africa	-35.0	-25.0	15.0	35.0		Africa	SUBTROPICAL
17	SAH	Sahara Desert	10.0	30.0	15.0	40.0		Africa	TROPICAL
18	AUS	Australia Continent	-40.0	-10.0	110.0	155.0		Australia	SUBTROPICAL
19	SEAS1	Southeast Asia Region 1	-10.0	20.0	75.0	105.0		Asia	TROPICAL
20	SEAS2	Southeast Asia Region 2	-10.0	20.0	105.0	135.0		Asia	TROPICAL
21	GOBI	Himalayas	37.5	47.5	85.0	112.5	>3000	Asia	TEMPERATE
22	EURAS	Eurasia Belt	40.0	60.0	30.0	90.0		Europe	TEMPERATE
23	SIB	Siberia	60.0	80.0	60.0	180.0		Asia	POLAR
24	NAK	New Alaska	45.0	60.0	170.0	195.0		N. America	BOREAL
25	MAINE	State of Maine	42.5	47.5	287.5	292.5		N. America	TEMPERATE
26	BOSTN	Boston, Massachusetts	40.0	42.5	290.0	292.5		N. America	TEMPERATE
27	NYC	New York, New York	40.0	42.5	287.5	290.0		N. America	TEMPERATE
28	OCNCY	Ocean City, Maryland	37.5	40.0	285.0	287.5		N. America	TEMPERATE
29	VABCH	Virginia Beach, Virginia	35.0	37.5	282.5	285.0		N. America	SUBTROPICAL
30	MYRBC	Myrtle Beach, South Carolina	32.5	35.0	280.0	282.5		N. America	SUBTROPICAL
31	JAX	Jacksonville, Florida	30.0	32.5	277.5	280.0		N. America	SUBTROPICAL
32	MIA	Miami, Florida	25.0	27.5	277.5	280.0		N. America	SUBTROPICAL

15

Table 4   Selected Areas-of-Interest

33	BURL	Burlington, New Hampshire	42.5	45.0	285.0	287.5		N. America	TEMPERATE
34	BUFF	Buffalo, New York	42.5	45.0	280.0	282.5		N. America	TEMPERATE
35	PITT	Pittsburgh, Pennsylvania	40.0	42.5	280.0	282.5		N. America	TEMPERATE
36	CHWV	Charleston, West Virginia	37.5	40.0	277.5	280.0		N. America	TEMPERATE
37	ASHVL	Asheville, North Carolina	35.0	37.5	275.0	277.5		N. America	SUBTROPICAL
38	ATL	Atlanta, Georgia	32.5	35.0	275.0	277.5		N. America	SUBTROPICAL
39	TALL	Tallahassee, Florida	30.0	32.5	272.5	275.0		N. America	SUBTROPICAL
40	COL	Columbus, Ohio	37.5	40.0	275.0	277.5		N. America	TEMPERATE
41	NASH	Nashville, Tennessee	35.0	37.5	272.5	275.0		N. America	TEMPERATE
42	JACMS	Jackson, Mississippi	30.0	32.5	267.5	270.0		N. America	SUBTROPICAL
43	DUL	Duluth, Minnesota	45.0	47.5	265.0	267.5		N. America	TEMPERATE
44	CHI	Chicago, Illinois	40.0	42.5	270.0	272.5		N. America	TEMPERATE
45	KC	Kansas City, Missouri	37.5	40.0	265.0	267.5		N. America	TEMPERATE
46	DAL	Dallas, Texas	32.5	35.0	262.5	265.0		N. America	SUBTROPICAL
47	SF	San Francisco, California	37.5	40.0	237.5	240.0		N. America	SUBTROPICAL
48	LA	Los Angeles, California	32.5	35.0	240.0	242.5		N. America	SUBTROPICAL
49	PORT	Portland, Oregon	45.0	47.5	235.0	237.5		N. America	TEMPERATE
50	SPOK	Rocky Mountains	47.5	50.0	240.0	242.5	>2000	N. America	TEMPERATE
51	BOIS	Boise, Idaho	42.5	45.0	242.5	245.0		N. America	TEMPERATE
52	HAWNV	Hawthorne, Nevada	37.5	40.0	240.0	242.5		N. America	SUBTROPICAL
53	LASV	Las Vegas, Nevada	35.0	37.5	242.5	245.0		N. America	SUBTROPICAL
54	TUCS	Tucson, Arizona	30.0	32.5	247.5	250.0		N. America	SUBTROPICAL
55	CCUT	Cedar City, Utah	35.0	37.5	245.0	247.5		N. America	SUBTROPICAL
56	LIVMT	Livingston, Montana	45.0	47.5	247.5	250.0		N. America	TEMPERATE
57	RSWY	Rock Spring, Wyoming	40.0	42.5	250.0	252.5		N. America	TEMPERATE
58	CSOO	Rocky Mountains	37.5	40.0	252.5	255.0	>2000	N. America	TEMPERATE
59	ALBQ	Albuquerque, New Mexico	32.5	35.0	252.5	255.0		N. America	TEMPERATE
60	LAR	Laredo, Texas	27.5	30.0	260.0	262.5		N. America	SUBTROPICAL
61	HAAM	Himalayas	32.5	42.5	245.0	257.5	>3000	Asia	TEMPERATE
62	NDSD	North & South Dakota	42.5	50.0	255.0	265.0		N. America	TEMPERATE
63	WCUS	West Cost US: Washington & Oregon	42.5	50.0	235.0	240.0		N. America	TEMPERATE
64	DC	Washington, D.C.	35.0	40.0	280.0	285.0		N. America	TEMPERATE
65	NWAFR	West Africa: Northwest Coast	2.5	17.5	340.0	355.0		Africa	TROPICAL

Table 4 Selected Areas-of-Interest

66	MOR	Northwest Africa: Morocco	30.0	37.5	352.5	357.5			Africa	SUBTROPICAL
67	GRAUS	Greater Australia Continent	-30.0	-10.0	110.0	160.0			Australia	TROPICAL
68	NAUS	Northern Australia: Tanami Desert	-25.0	-15.0	130.0	137.5			Australia	TROPICAL
69	ANT	Antarctic Circle	-90.0	-65.0	0.0	360.0			Antarctic	POLAR
70	NCHD	Northern China Desert	35.0	47.5	75.0	95.0			Asia	TEMPERATE
71	WIC	Arabian Sea	10.0	25.0	60.0	75.0			WATER/Mlo	TROPICAL
72	HIM	High Altitude Area in Asia: Himalayan	20.0	30.0	60.0	90.0			Asia	TEMPERATE
73	KJ	Far East: Korea & Japan	30.0	45.0	125.0	140.0			Asia	TEMPERATE
74	ME	Middle East	25.0	40.0	45.0	65.0			Asia	SUBTROPICAL
75	CHAG	South America: Chile & Argentina	-55.0	-35.0	285.0	295.0			S. America	SUBTROPICAL
76	EBRZ	East Coast of Brazil	-30.0	-10.0	310.0	325.0			S. America	TROPICAL
77	WSAM	West Coast of South America	-30.0	0.0	277.5	295.0			S. America	TROPICAL
78	NSAM	Northern Tip of South America	-12.5	-7.5	282.5	300.0			S. America	TROPICAL
79	WMEX	West Coast of Mexico	20.0	32.5	242.5	250.0			N. America	TROPICAL
80	NALAS	North America: Alaska State	57.5	75.0	195.0	225.0			N. America	POLAR
81	NCAN	Northern Canada	60.0	75.0	230.0	300.0			N. America	POLAR
82	GRNL	Greenland	60.0	85.0	290.0	350.0			Greenland	POLAR
83	WRUS	Western Russia: Moscow Vicinity	50.0	65.0	20.0	60.0			Europe	TEMPERATE
84	ERUS	Eastern Russia	45.0	70.0	80.0	130.0			Asia	BOREAL
85	POL	Pacific Ocean: Polynesian Islands	-30.0	10.0	180.0	230.0			WATER/Pac	TROPICAL
86	AHAGR	Ahaggar, Algeria	22.5	25.0	5.0	7.5	>1000		Africa	SUBTROPICAL
87	ALBRTA	Alberta, Canada (Rockies)	52.5	55.0	240.0	245.0	>1000		N. America	TEMPERATE
88	ALPS	Alp Mountains	45.0	47.5	5.0	10.0	>1000		Europe	TEMPERATE
89	ANTHI	Antartica	-85.0	-72.5	10.0	122.5	>3000		Antarctic	POLAR
90	AQUAS	Aguas, Mexico	22.5	25.0	257.5	260.0	>1000		N. America	TROPICAL
91	ECONGO	East Congo (Zaire)	-7.5	5.0	27.5	30.0	>1000		Africa	TROPICAL
92	ETHIOP	Ethiopia	0.0	7.5	40.0	42.5	>2000		Africa	TROPICAL
93	GRNLHI	Greenland	67.5	70.0	320.0	325.0	>3000		Greenland	POLAR
94	GRNLN	Greenland (North)	72.5	80.0	320.0	330.0	>2000		Greenland	POLAR
95	GRNLS	Greenland (South)	62.5	67.5	310.0	320.0	>2000		Greenland	POLAR
96	HUANCO	Huancayo, Peru (Andes)	-12.5	-10.0	285.0	287.5	>3000		S. America	TROPICAL
97	IRKTSK	Irkutsk, Siberia	50.0	55.0	97.5	102.5	>1000		Asia	BOREAL
98	KABUL	Kabul, Afghanistan	32.5	35.0	65.0	67.5	>2000		Asia	SUBTROPICAL

Table 4   Selected Areas-of-Interest

99	KASHMR	Kashmir, India (Himalayas)	32.5	35.0	75.0	77.5	>5000	Asia	TEMPERATE
100	LAPAZ	LaPaz, Bolivia (Andes)	-20.0	-15.0	290.0	292.5	>4000	S. America	TROPICAL
101	LHASA	Lhasa, Tibet (Himalayas)	30.0	32.5	90.0	92.5	>5000	Asia	TEMPERATE
102	LNZHU	Lanzhou, China	35.0	37.5	100.0	102.5	>2000	Asia	TEMPERATE
103	NGUIN	New Guinea	-5.0	-2.5	140.0	142.5	>1000	WATER/Pac	TROPICAL
104	PYRNES	Pyrenee Mountains	42.5	45.0	357.5	2.5	>1000	Europe	SUBTROPICAL
105	QUITO	Quito, Ecuador (Andes)	0.0	2.5	282.5	285.0	>1000	S. America	TROPICAL
106	SANTGO	Santiago, Chile (Andes)	-32.5	-30.0	287.5	290.0	>1000	S. America	SUBTROPICAL
107	TANGMI	Tangmai, Tibet	27.5	30.0	92.5	100.0	>4000	Asia	TEMPERATE
108	TEHRAN	Tehran, Iran	32.5	35.0	50.0	52.5	>2000	Asia	SUBTROPICAL
109	URALS	Ural Mountains	57.5	62.5	57.5	62.5	>1000	Europe	BOREAL
110	XINING	Xining, China (Himalayas)	35.0	37.5	102.5	105.0	>3000	Asia	TEMPERATE
111	ATL00C	Atlantic North Central Equator	0.0	10.0	335.0	345.0		WATER/Atl	TROPICAL
112	ATL10C	Atlantic North Central 10 lat	10.0	20.0	315.0	330.0		WATER/Atl	TROPICAL
113	ATL20C	Atlantic North Tropic of Cancer	20.0	30.0	315.0	325.0		WATER/Atl	SUBTROPICAL
114	ATL30C	Atlantic North Central 30 lat	30.0	40.0	310.0	330.0		WATER/Atl	SUBTROPICAL
115	ATL40C	Atlantic North Central 40 lat	40.0	50.0	320.0	335.0		WATER/Atl	TEMPERATE
116	ATL50	GIUK (Grnland, Iceland, UK)	50.0	60.0	320.0	340.0		WATER/Atl	TEMPERATE
117	ATLS2	Atlantic South (Ascension Ilse)	-10.0	0.0	340.0	350.0		WATER/Atl	TROPICAL
118	ATLS4	Atlantic South (Trnidade Brazil Ilse)	-30.0	-15.0	325.0	335.0		WATER/Atl	TROPICAL
119	ATLS6	Atlantic South (Nightingale Ilse)	-40.0	-35.0	340.0	5.0		WATER/Atl	SUBTROPICAL
120	BANGK	Bangkok, Thailand	10.0	12.5	100.0	102.5		Asia	TROPICAL
121	BAGDAD	Baghdad, Iraq	32.5	35.0	42.5	45.0		Asia	SUBTROPICAL
122	JAPSEA	Korea & Japan (Lower Sea of Japan)	32.5	40.0	125.0	137.5		Asia	TEMPERATE
123	CAPTOW	Cape Town, South Africa	-35.0	-32.5	17.5	20.0		Africa	SUBTROPICAL
124	MOSCOW	Moscow, Russia	55.0	57.5	37.5	40.0		Europe	TEMPERATE
125	PEILSE	Prince Edward Island, Canada	45.0	47.5	295.0	297.5		N. America	TEMPERATE
126	MANAUS	Manaus, Brazil (Amazon Forest)	-5.0	-2.5	297.5	300.0		S. America	TROPICAL
127	NEWCAL	New Caledonia	-20.0	-17.5	165.0	167.5		Asia	TROPICAL
128	NEWZEA	New Zealand	-45.0	-42.5	170.0	172.5		Asia	TEMPERATE
129	RIODEJ	Rio de Janerio	-25.0	-22.5	315.0	317.5		S. America	TROPICAL
130	FALKLD	Falklands	-52.5	-50.0	300.0	302.5		S. America	TEMPERATE

18

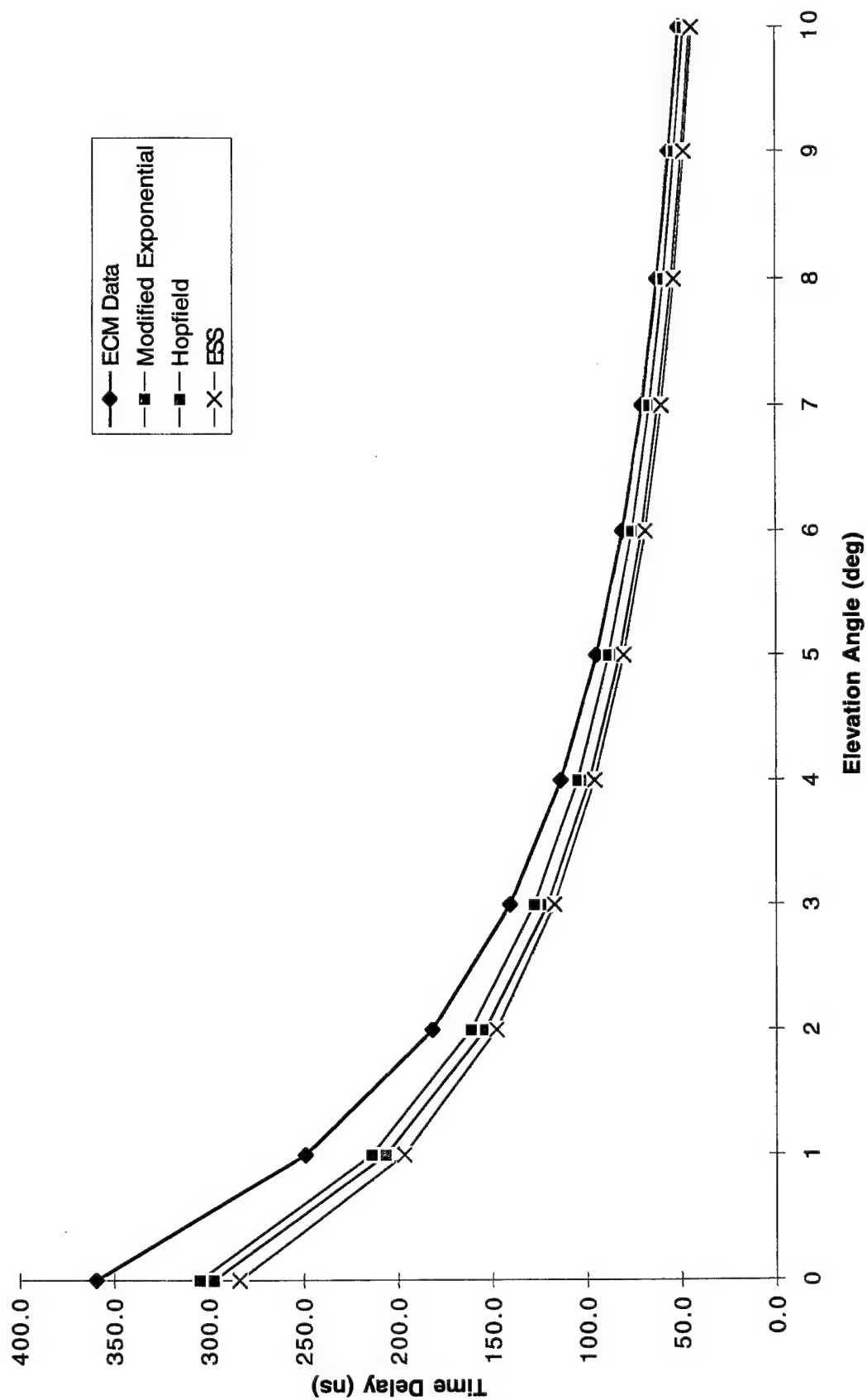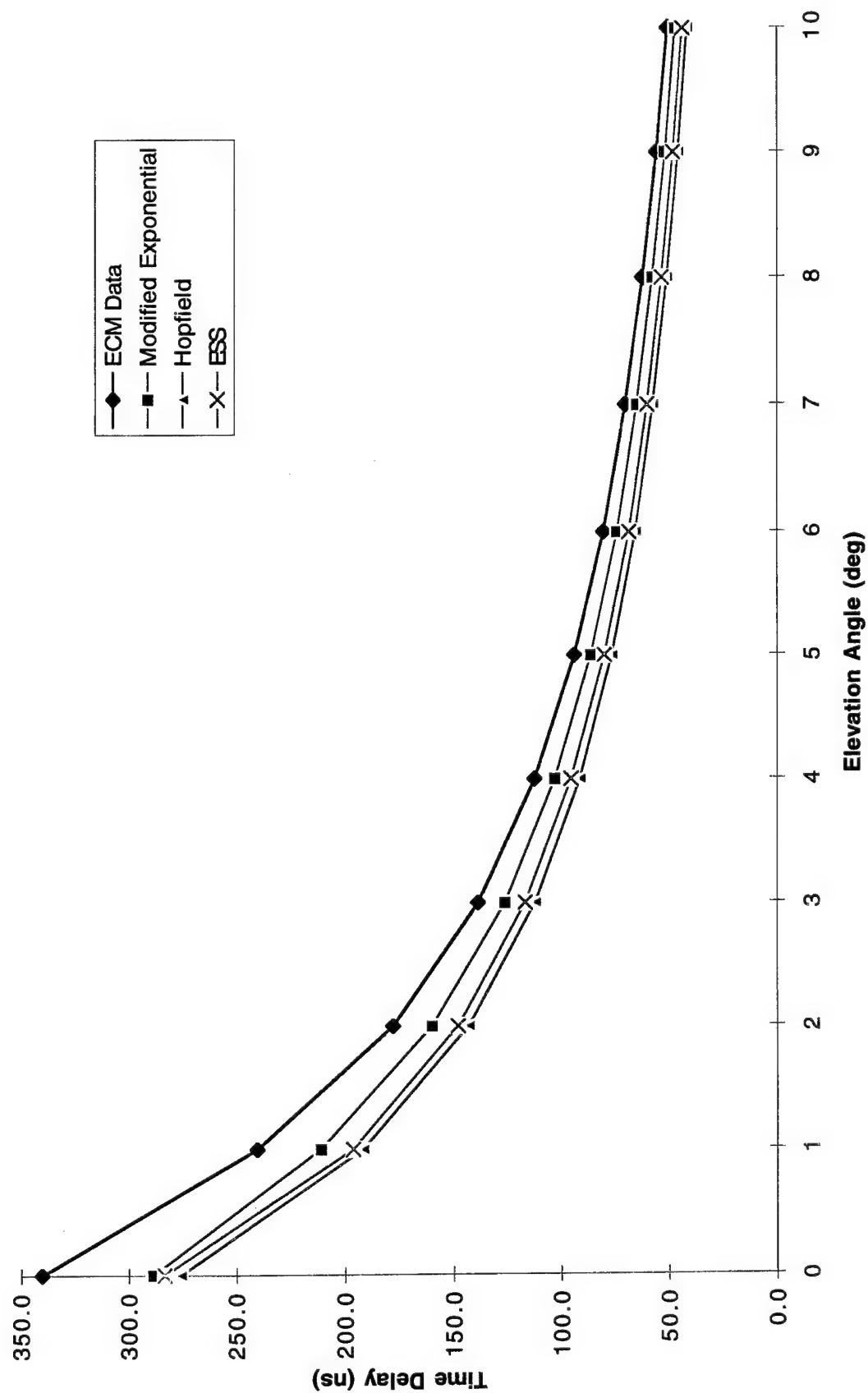Figure 6. Time Delay vs. Elevation Angle Tehran, Iran (February, ECMWF Data)

19

Figure 7. Time Delay vs. Elevation Angle Tehran, Iran (August, ECMWF Data)

4.2. Error Parameter Statistics

Particular interest to this project is the derivation of time delay, range error, and angle of arrival error for positive elevation angle and negative elevation angle from the horizontal direction. Also the standard deviations of each error parameters are derived. The calculation method of standard deviation is discussed below. In addition, azimuth sensitivity is analyzed.

4.2.1. Time Delay, Range Error, and Angle of Arrival Error for Negative Elevation

In a satellite communication sytem, the transmitter or receiver antenna of the ground stataton transmits or receives signal above 90 degree form zenith angle or negative angle from horizental direction. The modified exponential tropospheric model generates time delay, range error, and angle of arrival error for any negative elevation angle between a ground station and satellite station. Figure 8a, 8b, and 8c show the ECMWF worldwide contour maps of time delay, range error, and angle of arrival error for 90.5 degree zenith angle as an example.

4.2.2. Standard Deviations

Percent standard deviations are calculated for time delay and zenith launch angle for each of the 10,368 grids. For each grid TD_{1i}, ray traces were run for the target grid and surrounding grids with the grid crossing feature turned off. Table 5 shows grid time delays required to calculate standard deviation for TD1.

Table5. Sample Grid for Standard Deviation Calculation

TD2	TD3	TD4
TD5	TD1	TD6
TD7	TD8	TD9

First, the time delay is determined for each of the surrounding grids. Then the average and standard deviation is calculated for TD1i:

$$TD_{avg} = \sum_{i=1}^{m} TD_i \ / \ m$$

$$TD_{var} = \sum_{i=1}^{m} (TD_i - TD_{avg})^2 \ / \ m - 1$$

21
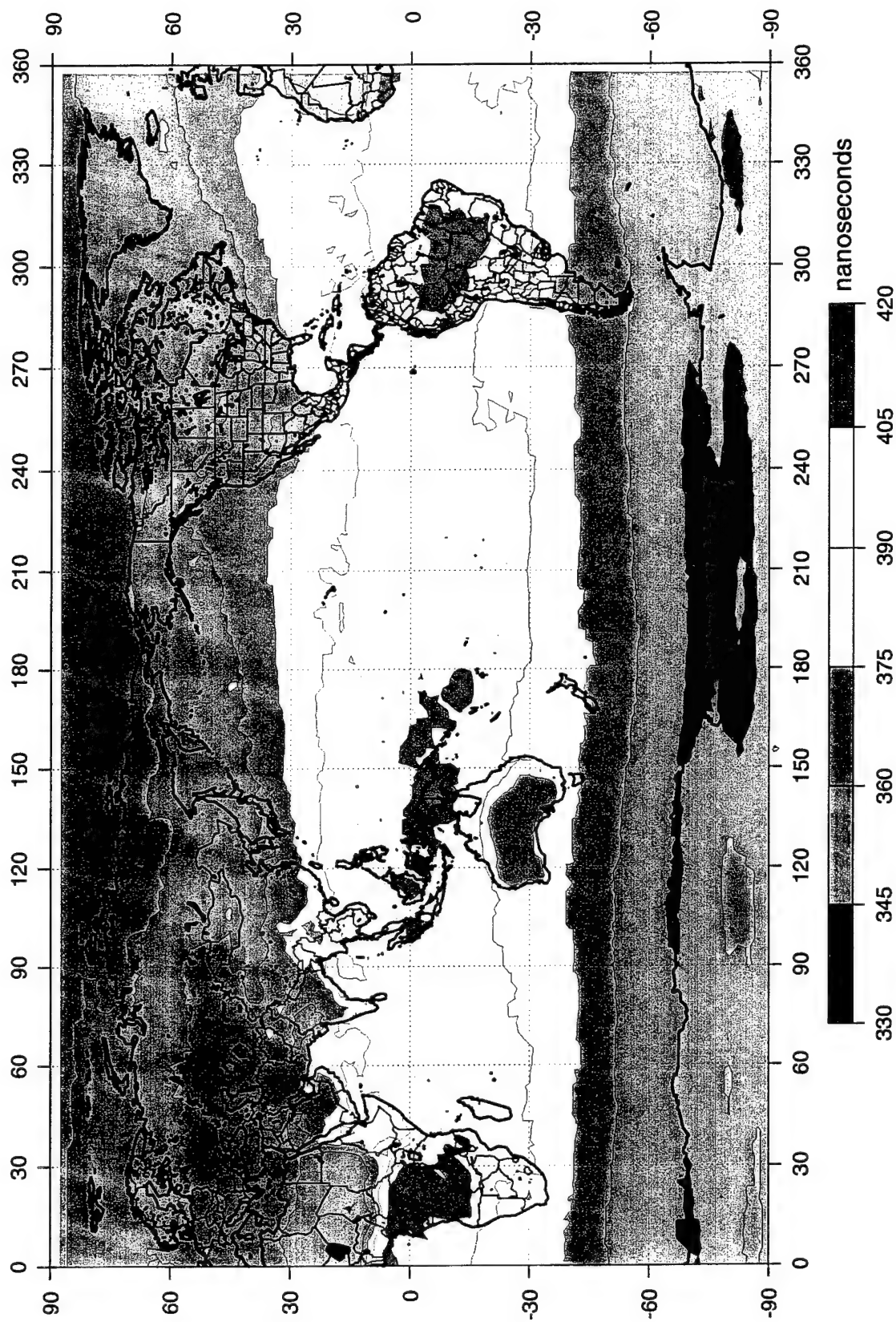
Figure 8a -ECMWF Time Delay Contour Map for March , Truezenang = 90.5 deg.

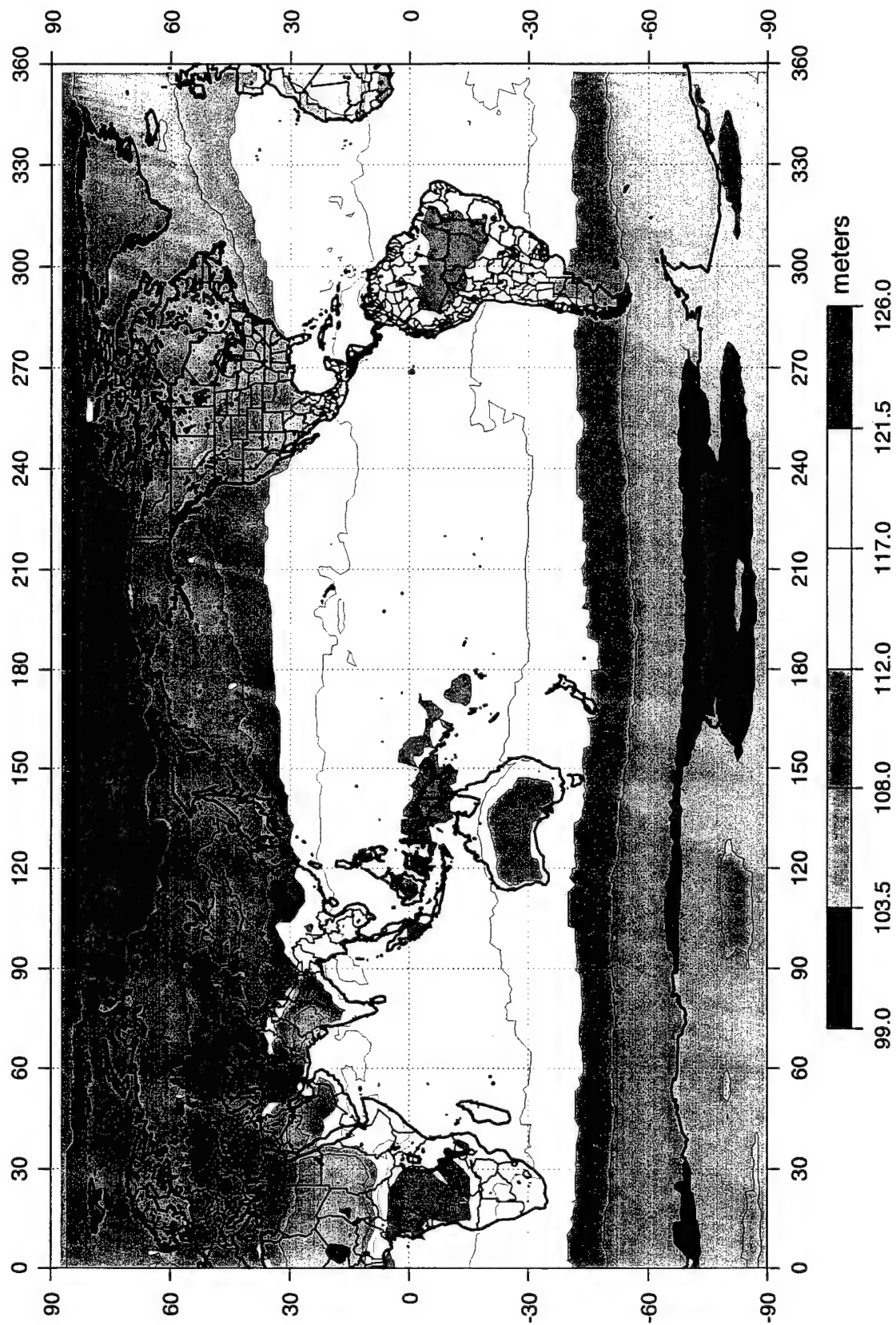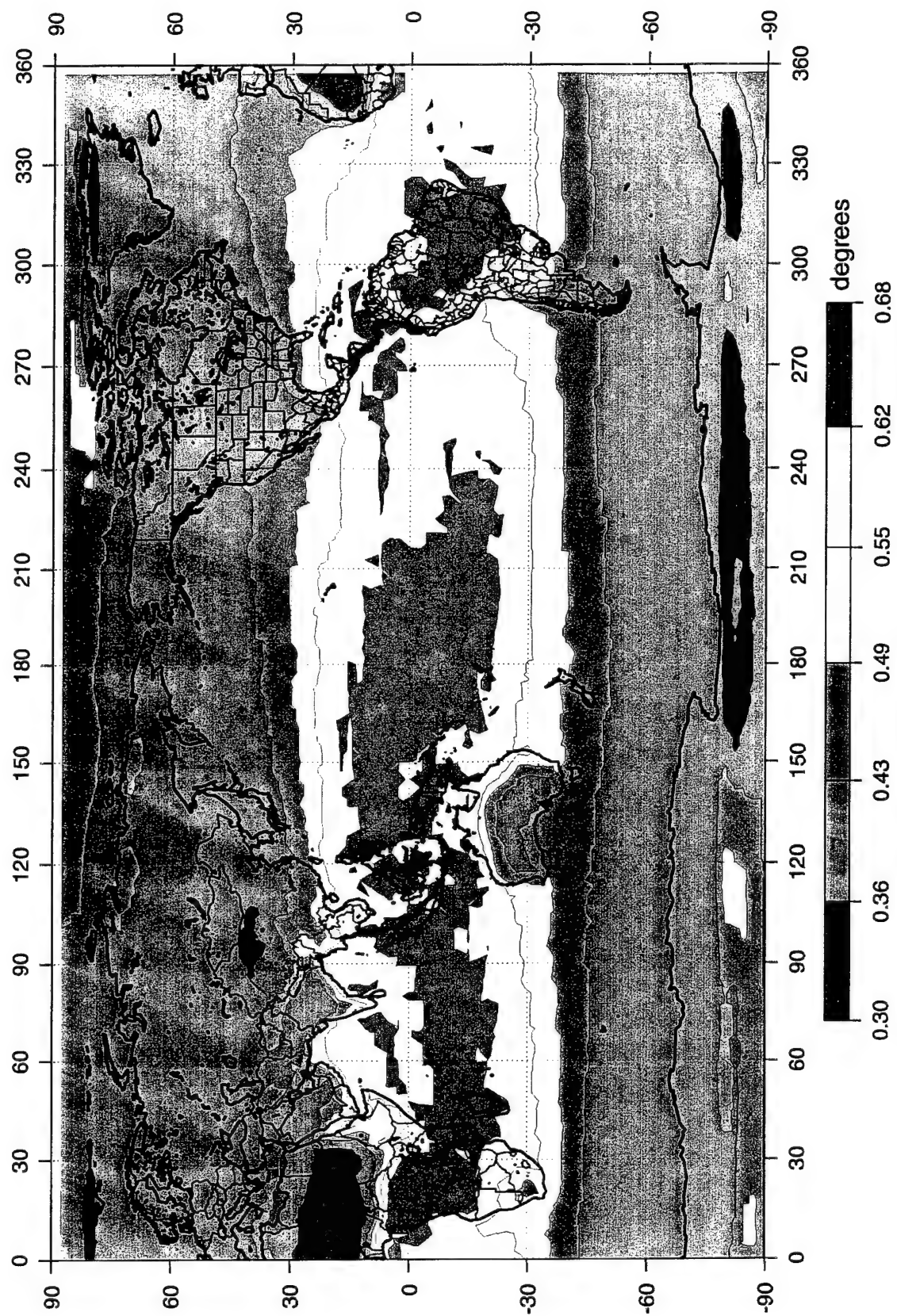Figure 8b -ECMWF Range Error Contour Map for March , Truezenang = 90.5 deg.

meters

99.0 103.5 108.0 112.0 117.0 121.5 126.0

Figure 8c - ECMWF Angle of Arrival Error Contour Map for March , Truezenang = 90.5 deg.

degrees

0.30 0.36 0.43 0.49 0.55 0.62 0.68

$$TD_{stdev} = \sqrt{TD_{var}}$$

where m is 9 (plus or minus one surrounding grid) for grids between 60° North and 60° South in latitude. For latitudes between 60° and 70° North/South, plus or minus two grids from the center grid covers 25 grids. For latitudes between 70° and 80° North/South, plus or minus three grids from the center of grid covers 49 grids. For latitudes between 80° and 90° North/South, plus or minus four grids form the center of grid covers 81 grids. Next, percent standard deviation is taken by dividing the standard deviation by the original time delay and multiplying by 100.

$$\% \text{ StDev} = (TD_{stdev} / TD1) * 100$$

These calculations are performed for all grids for 12 months using ECMWF data and HIRAS data. Appendix D show contour plots of percent standard deviation for time delay using ECMWF data.

4.2.3. Azimuth Sensitivity

The time delay is calculated for every other grid of the 10,368 grids. Time delay for the case of azimuth independent is compared with that of azimuth dependent. The range between minimum and maximum time delays for the azimuth dependent case is about 45 % of those in the azimuth independent case. Contour maps for azimuth sensitivity referencing data and HIRAS data are shown in appendix E respectively.

5. VALIDATION OF THE MODIFIED EXPONENTIAL MODEL CODE

The modified exponential model code is designed as a subroutine package which can be incorporated into an application. All code is written in ANSI-standard FORTRAN 77 with no machine-dependent extensions except VAX system (the data files in VAX system need a special format for direct access data). This program is divided into two major subroutine. One is I/O subroutine(getwxfil) and the other is the main calculation routine(raytrace). These two main subroutines are further divided into two subroutines in order to calculate time delay, range error, and angle of arrival error.

The tropospheric model code would invoke the user information and user request database. Then, it will proceed to call main calculation routine with user information. This model program will generate error or status messages to validate each subroutine and function. If an error or a status flag is returned from a subroutine or function, the troposphere program will terminate or return an error message indicating the subroutine where it was generated.

5.1. Main Program

The main program initializes and defines variables needed in I/O subroutine and raytrace calculation subroutine. I/O subroutine reads two data files. One contains weather data containing grid number, latitude, longitude, surface refractivity, pressure, temperature, and undulation of geoid parameter. The other contains reference height coefficient for each $2.5° \times 2.5°$ degree grid. The user can choose one option whether grid cross or without grid cross features. If the grid cross feature contains new grid information (surface refractivity, pressure, and temperature) of a ray path crossing, new grid information rather than previous grid information will be used to calculate the refractivity with its respective height. If a ray path crosses more than two grids, raytrace subroutine will repeat above process to calculate time delay, range error, and angle of arrival error. Raytrace subroutine will use the arguments passed from the main routine to generate time delay, range error, and angle of arrival error. The mathematical equations used for this routine are described in section 5.3. The user input is as follows:

(Q) Enter the grid cross feature (0 : without grid cross, 1 : with grid cross)

(O) Enter Source option (1, 2, 3, or 4)

      1. ECM database
      2. MRF database
      3. HIRAS database
      4. User database

(Q) Enter the location of station (latitude, longitude)

(Q) Enter month, day or time

(Q) Enter the station height

(Q) Enter the Elevation angle (0 ~ 90 degree)

(Q) Enter the azimuth angle

If the user does not set the geophysical parameters and specified date for the tropospheric model by passing calling arguments to I/O subroutine and raytrace subroutine, error messages will be displayed and will prompt input questions to validate feature, option, and other previously inputted informations. Figure 9 and 10 show the syntax for the interface and describe calling arguments.

5.2. Input & Output Subroutine

Figure 11 is a diagram of the subroutine which makes up the I/O routine. If the user selects "ECM or HIRAS or MRF database" source and without grid cross feature,

call getwxfil (GCrossFlg, Source, Lat, Lon, Press, Temp, RelHum, MslFlg, Mon, Hour, *Day, Yr*, LFCtropo1, LFCtropo2, Dataray, Datarayflg)

INPUTS:

GCrossFlg	(Integer*2)	0--Disable Grid Crossing feature
		1--Enable Grid Crossing feature
Source	(integer*2)	Data Source
		1--ECM
		2--MRF
		3--Hiras
		4--User
Lat	(real*8)	(Latitude -90 to +90)
Lon	(real*8)	(Longitude 0 to 360 or -180 to +180)
[1] Press	(real*8)	Surface Pressure (mbars)
[2] Temp	(real*8)	Surface Temperature (°K)
[3] RelHum	(real*8)	Surface Relative Humidity (%)
MslFlg	(integer*2)	Reference
		0--Ellipsoid
		1--Mean Sea Level (Default)
Mon	(integer*2)	Month (1 to 12)
Hour	(integer*2)	Hour 1--0000Hrs
		2--0600Hrs
		3--1200Hrs
		4--1800Hrs
Day	(integer*2)	Day 1 to 31
Yr	(integer*4)	Year 1991, 1992,etc.
LFCtropo1	(integer*2)	Logical File Code 1 (Unit number)
LFCtropo2	(integer*2)	Logical File Code 2 (Unit Number)

OUTPUTS:

Dataray	(real*8)	array(0:730,1:7)
		(grid)
		(lat)
		(lon)
		(refractivity)
		(Height Coefficient)
		(Range Error Variance)
		(Angle of Arrival Error Variance)
DatarayFlg	(integer*2)	Error flag
		0--No error during data retrieval
		1--Error during data retrieval

NOTE: Superscript [1,2,and 3] are for input for source 4 and Output for data source ECMWF, MRF, and HIRAS.

Figure 9. I/O routine syntax and calling arguments

call raytrace (MslFlg, TrueZenAng, TropoHgt, StnAlt, Az, RangeSat, c, freq, Dataray, GCrossFlg, STDFlg, TimeDelay, TimeDelaySTD, ZenLnchAng, ZenLnchAngSTD, RngDelay, RngDelaySTD, ErrFlg,DiffRange)

INPUTS:

MslFlg	(integer*2)	Reference
		0--Ellipsoid
		1--Mean Sea Level (Default)
TrueZenAng	(real*8)	Zenith angle to line of site
TropoHgt	(real*8)	Height of Troposphere (Default 27 km)
StnAlt	(real*8)	Station Altitude (m)
Az	(real*8)	Azimuth angle(0 ~ 360)
RangeSat	*(real*8)*	*Range site to receiver (Not used currently)*
c	(real*8)	Speed of light in Vacuum
freq	*(real*8)*	*Frequency (Not used currently)*
Dataray	(real*8)	array(0:730,1:7)
		(grid)
		(lat)
		(lon)
		(refractivity)
		(Height Coefficient)
		(Range Error Variance)
		(Angle of Arrival Error Variance)
GCrossFlg	(Integer*2)	0--Disable Grid Crossing feature
		1--Enable Grid Crossing feature
STDFlg	(Integer*2)	0--No Standard Deviation desired
		1--Standard Deviation desired

OUTPUTS:

TimeDelay	(real*8)	Time Delay (ns)
TimeDelaySTD	(real*8)	Time Delay Variance (ns^2)
ZenLnchAng	(real*8)	Zenith Launch Angle (Antenna pointing angle)
ZenLnchAngSTD	(real*8)	Zenith Launch Angle Variance (deg^2)
RngDelay	(real*8)	Range Error (m)
RngDelaySTD	(real*8)	Range Error Variance (m^2)
ErrFlg	(integer*2)	Error flag
		0--No error during raytrace
		1--Error during draytrace
DiffRange	*(real*8)*	*Range difference exiting troposphere(m)*
		(Not used currently)

NOTE: *Italic Letter is not used currently*

Figure 10. Raytrace routine syntax and calling arguments

Figure 11 Diagram of I/O subroutine
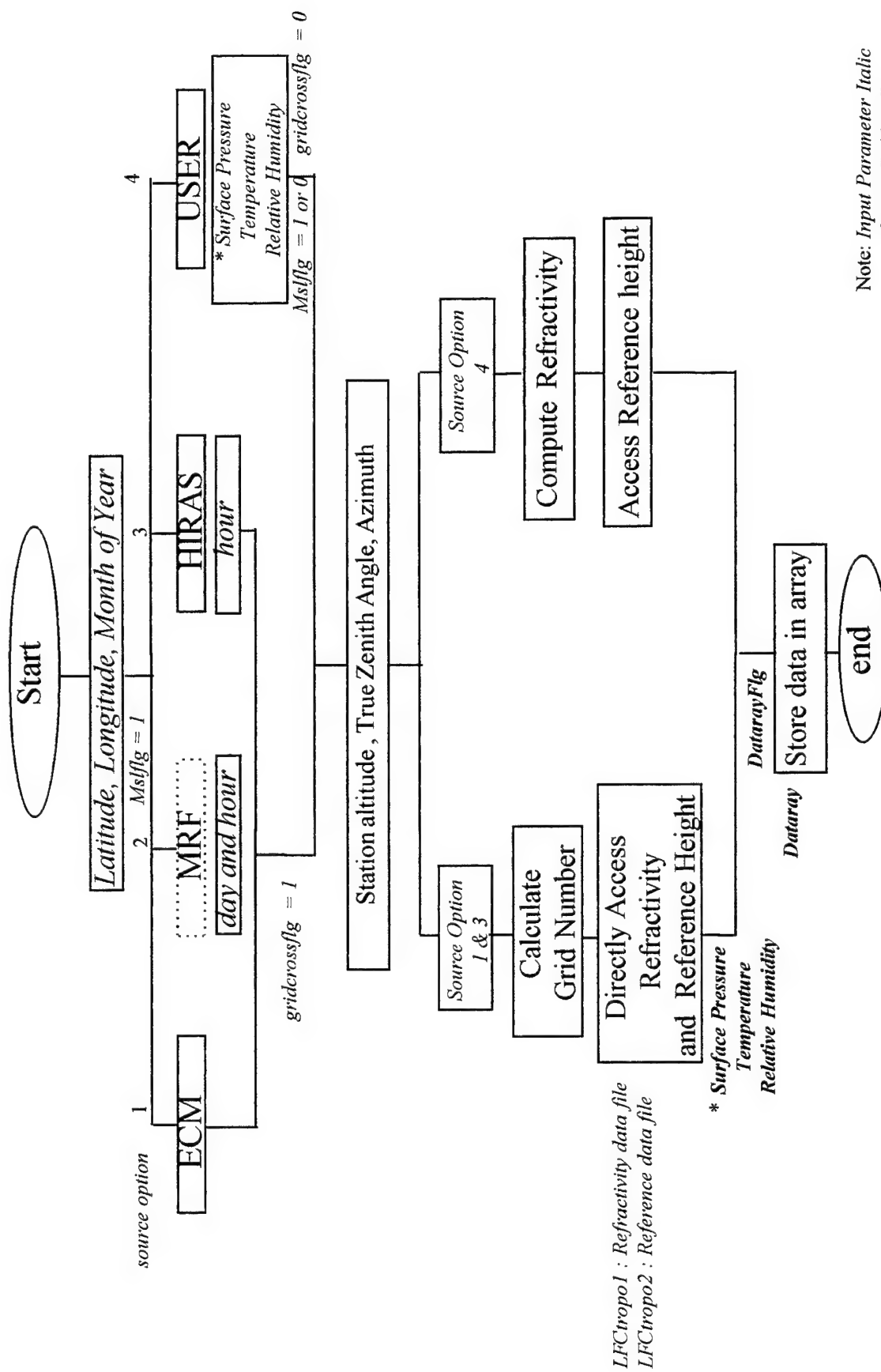
this routine calls grid calculating function. If the returned grid from the grid calculation function is out of range, the program will terminate. If not, grid number will go to the data accessing subroutine to extract user's desired data with respect to grid number. In order to test whether the user chooses the right one, I/O subroutine generates print statement for verification of I/O status. When opening files successfully accesses to the desired data, the IOSTAT identity in the read statement indicates whether the file has been successfully opened. If no error message is returned, the selected data is stored in an array. Thus, I/O routine uses dynamic memory allocation method based on specified geographic location for data storage. Table 6 shows dynamic memory allocation size for the geophysical location.

A ray path at $0°$ elevation angle indicates the maximum distance from ground station to the target or the spacecraft. A ray path distance to the top of troposphere (27 Km from the surface) is approximately 587.49 Km at $0°$ elevation angle. In table 6, we can see the different memory size based on latitude. For example, the user selects the latitude range between 60 ~ -60 degree, I/O program allocates array size (9,13). If the user selects "User database" source, this calls user_info subroutine that returns surface pressure, temperature, and humidity needed to generate surface refractivity.

Table 6. Memory allocation for different latitude

Latitude	Memory Size Note: First parameter refers to latitude for grid. Second refers to longitude for grid.
80 ~ 90 degree	array (9, 73)
70 ~ 80 degree	array (9, 25)
60 ~ 70 degree	array (9, 17)
60 ~ -60 degree	array (9, 13)
-60 ~ -70 degree	array (9, 17)
-70 ~ -80 degree	array (9, 25)
-80 ~ -90 degree	array (9, 73)

If inputs are invalid, the routine will be run out of range error message. Given that all inputs are valid, I/O routine reads reference coefficient height with respect to input.

Each subroutine is validated by using example. The function of each subroutine is as follows:

a.user_info

This subroutine calls cal_refrac subroutine that calculates surface refractivity and reads reference coefficient height data file containing the undulation parameter of geoid and reference coefficients height. There are two different version (SUN and VAX). In SUN version, the operation system type parameter(ostype) is equal "sun", reads the data file (refht/refht.new) under user's installed path. In VAX version, reads the data file ([.refht]refht.vax). In order to validate whether reading user's desired data file or not, added printer statement.

Inputs are LFCtropo1, mslflg, ostype, date, latitude, longitude, pressure, temperature, and relative humidity. Refractivity and reference height are stored in an array, dataray. Dataray and datarayflg (error flag) are passed out. Validation input, expected output and actual output from subroutine are :

Input (lat, lon)	Expected Grid Number	Output from subroutine
23.5 33.7	1310	1310
-23.5 -33.7	6467	6467
33.6 226.6	1963	1963

b. cal_refrac

This subroutine calculates surface refractivity. The refractivity for air which contains water vapor is given as

$$N = \frac{77.6 * p}{T} + \frac{e * 3.73 \times 10^5}{T^2}$$

e : water vapor
p : atmosphere's barometric pressure
T : atmosphere's temperature.

The first part of the right hand side of the equation computes dry refractivity. The second part computes wet refractivity. Inputs are surface pressure, temperature, and relative humidity. Output is the total surface refractivity.

31

c. direct_access

This subroutine reads data files, and then accesses data directly to datafiles. Inputs are cm, source, ostype, grid, date, LFCtropo1, LFCtropo2. Output parameter is called as parm array. In order to validate direct_access subroutine, inputs are passed through user_info subroutine and outputs are stored in parm array. When the input and output data with respect to user's input do not match , for example, the input grid number is not equal to the output grid number, I/O read or open file error messages are displayed and terminate program.

d. grabGrid

This subroutine organizes an array of data, dataray, in an organized manner. The organization allows for faster reading of data files by creating a spread sheet that stores grids surrounding initial input position point. Grids are stored in an array that surrounds the position point in the counterclockwise direction. Grids spread outward from initial point in rings which are in odd square matrix. In cases where initial position lies between 70 and 80 degrees latitude, the grids spread in odd square matrix up to four rings then spreads further in longitude direction adding six columns of grids to the right and left of the square. The additional columns accounts for the increased possibility of grid crossing. Inputs are cm, date, azimuth, LFCtropo1, LFCtropo2, mslflg, latitude, longitude, source, ostype, pressure, temperature, relative humidity. Outputs are dataray and datarayflg.
Table 7 shows the result of validation for storing data in an array to different user input. The array size are relative with respect to table 6 in section 5.2.

Table 7 Dynamic memory allocation of different user input

33					27
15	14	13	12	11	
16	4	3	2	10	
17	5	Input	1	9	25
18	6	7	8	24	
19	20	21	22	23	
39					45

Note : Each number represents the array index.

5.3. Raytrace Subroutine

There are three main parts in the raytrace subroutine. Figure 12 shows a diagram of the raytrace subroutine. Part one is an iterative approach used to compute the aggregate refractive effect of radio propagation from ground station to the top of troposphere (27 Km from the surface). Given a specific refractivity-height profile, a ray path with increasing elevation angles are 'traced' up to the top of troposphere. Geometric techniques are then used to compute the true elevation angle given initial LOS angle. An initial estimate of the actual signal elevation angle is obtained by adding an angle of arrival error which was computed through the assumption that LOS angle is an initial true elevation angle. Snell's law for spherical geometry together with the refractivity height profile may now be used to compute a distance of ray path at each height in the troposphere.

The basic assumption is that the troposphere is considered to be stratified into m height profiles and constant refractivity profile N_m. In this subroutine, the height profiles is created by

0	~	1,000 meters	:	increment	100 meters
1,000	~	10,000 meters	:	increment	500 meters
10,000	~	top of troposphere	:	increment	1,000 meters.

Using the refractivity and the height profiles reaching up to the tropospheric height, a ray path in the troposphere can be obtained using Snell's law and Bouger's rule for spherical geometry as shown in the following:

$$\frac{\sin I_0}{r_0} = \frac{\sin\left[\frac{\pi}{2} + \alpha_0\right]}{r_1} \quad \text{and}$$

$$n_0 \, r_0 \cos \alpha_0 = n_1 \, r_1 \cos \alpha_1$$

where r_0 is the radius of the Earth, $r_1 = r_0 + h_0$, n is the radio refractive index of the atmosphere at any layer, and α is the apparent elevation angle for each refractive index profile, and I is an incident angle between different two layers. The ray path computed at each height of the troposphere can be used to compute the range using refractive bending of the ray. The range error equation is

$$\Delta R = \sum_{j=0}^{n} n_j \, R_j - R_{0m}$$

33

Figure 12 Diagram of Raytrace subroutine

Start

Input Parameters from Main/IO Routine

*MslFlg = 0 or 1,   TrueZenith Angle , Tropo Height = 27 Km(default)
Station altitude, Azimuth, Range satellite, Speed of light , Frequency,
Dataray, GcrossFlg, STDFlg*

ErrorFlg Calculate Zenith Launch Angle

Different Range

GcrossFlg   0

1

Determine Height of first grid crossing

ErrorFlg

Calculate positions of grid crossing

ErrorFlg

Calculate each Refractivity

Calculate Each Refractivity

STDFlg   0   1

Calculate Time Delay,Range Delay

*Time Delay
Zenith Lach Angle
Range Delay*

Calculate Time Delay,Range Delay Standard Deviation

*Time Delay STD
ZenLnchAng STD
Range STD*

End

Note: *Input Parameter Italic*

Output Bold Italic

34

where the distance R_j is given by

$$R_j^2 = r_j^2 + r_{j+1}^2 - 2\ r_j\ r_{j+1}\ \cos\theta_j$$

and the distance R_{0m} is

$$R_{om} = r_0^2 + r_{m+1}^2 - 2\ r_0\ r_{m+1}\ \cos\left[\sum_{j=0}^{m}\theta\right]$$

and

$$\theta_j = \frac{\Pi}{2} - \alpha_j - i_j.$$

The refraction angle error $\Delta\alpha_m$, which is the difference between the apparent elevation angle and the LOS elevation angle, can then be determined from

$$\Delta\alpha_m = \alpha_0 - \alpha_{0m}.$$

Part one of the program uses many mathematical equations such as arccosine, arcsine, and square root function. In order to validate above mathematical equations, the value of arccosine and arcsine is assumed to be greater than 1. Then, it returns an out-of-range error message and resets the value to one. If the square root error occurs, the domain error message is returned and program will be terminated. Part two of the program uses climatology weather data to construct refractivity for each height profiles, defined in part one, based on surface data. In this part, it calculates each corner point on the grid which encloses the initial location. Then, finds the shortest perpendicular distance from initial location to grid lines. It calls position subroutine to find the last projected ground location to the top of tropospheric region. If the grid of the last location is equal to the initial grid, raytrace program will skip directly to part three of the program. If not, this part will check grid cross index. If the grid cross index is false, this part will be skipped and will proceed to part three. If the grid cross index is true, it will call position subroutine to find each projected location and grid number for each height profiles. If the grid number is not equal to initial grid, it will access surface refractivity for different grid number and compute refractivity with respect to height profile. This method to find each refractivity for height profile will be iterated until height reaches the troposheric location. Then refractivity will be passed into the third part of the program. The third part of program traces a ray from the Earth's ground surface to the top of troposphere and compute range error, time delay, and angle of arrival error.

a. position

This subroutine computes coordinates and distances for curved paths. This calls geodetic subroutine to convert given initial geodetic location to earth-center earth-fixed (ECEF) coordination. It calculates position vector (south, east, and zenith component) from the ground station to the satellite point using true elevation and azimuth. Adding geodetic vector to position vector returns a new vector position over the Earth. Then the routine calls *newwgs84latlon* subroutine to compute the subsatellite point on Earth's surface. The conversion of geodetic to geocentric coordination is described in appendix A. Inputs are gdlat1, gdlon1, alt1, az1, el1, hgo1. Outputs are new geocentric latitude and longitude.

b. newwgs84latlon

This subroutine computes WGS-84 geodetic latitude and longitude from ECEF coordinates. It computes initial geodetic latitude and longitude of subsatellite point. Then, it corrects the subsatellite point using four iteration loop. Input is ECF position, xecf. Outputs are geodetic subsatellite latitude "glat" degrees, geodetic subsatellite longitude "glon" degrees, altitude above ellipsoid "alt", and distance from the center of Earth to the surface point "rmag".

c. geodetic

This subroutine computes Earth-Centered Earth-Fixed (ECEF) cartesian coordinates given geodetic latitude, longitude and altitude. Inputs are geodetic latitude "xlat" in degrees, longitude "xlon" in degrees, and height "xh" above the reference ellipsoid in kilometers. Outputs are ECF x-coordinate "xx", y-coordinate "yy", z-coordinate "zz" in kilometers.

6. CONCLUSION

Four databases are selected as most valuable sources for climatological data. The 7 - variable surface data, is derived from the 17 variable multilayer data for use for the Modified Exponential Model. This model builds a multilayer atmosphere. The constructed atmospheric data are then used with Millman's Stratified layer method to calculate range error, time delay, and angle of arrival error. Tests performed on 130 various worldwide location indicate that most realistic results are obtained using the Modified Exponential Model. Numerous models are examined including Hopfield(with surface weather conditions) and ESS models. Error parameter statistics show that errors are less than six percent standard deviation in time delay and range error, with less than 24 percent standard deviation in zenith launch angle. In addition, azimuth sensitivity tends to be a function of location and time.

The Modified Exponential Model source code is created to be a user-friendly for the needs of radio propagation system engineer who need many propagation phenomena

analysis. Data files are provided in ASCII-format file and can be easily reformatted for direct-access. Although great care should be taken in modifying the program, the author would appreciate any comment regarding for improving the software quality.

ACKNOWLEGEMENTS

REFERENCES

1.   B.R. Bean and E.J. Dutton, "Radio Meteorology," National Bureau of Standards, Monograph 92, U.S. Government Printing Office, Washington, D.C., March 1966.

2.   K. Takahashi, "Atmospheric Error in Range and Range Rate Measurements Between a Ground Station and an Artificial Satellite," IEEE Trans. Aerosp. Electron. Syst. AES-6, 770-779 (1970)

3.   G.H. Millman, "Atmospheric Effects on Radiowave Propagation", in Modern Radar: Analysis, Evaluation, and Design," R.S. Berkowitz, edited, John Wiley & Sons, Inc., New York, 1965.

4.   H.S. Hopfield,"Two-quadratic Tropospheric Refractivity Profile for Correcting Satellite Data," J. Geophysics Research, (18), pp4487-4499 (1969).

5.   C.C. Goad and L.Gooddman, " A Modified Hopfield Tropospheric Refraction Correction Model," Proceedings of American Geophysics Union, Fall Annual Meeting, San Francisco, California, December 1974.

6.   T.D. Moyer, "Mathematical Formulation of the Double Precision Orbit Determination Program(DRODP)," Technical Report #32-1527, Jet Propulsion Laboratory, Pasadena, California, May 1971.

7.   T.E. Gallini, " A Survey of Tropospheric Refraction Models," #TOR-94(4488)-11, The Aerospace Corporation, El Segundo, California, April 1994.

Appendix A

Conversion Geodetic to Earth-Center Earth-Fixed (ECEF)

There are two most commonly used definitions of latitude. Figure 13 shows Geocentric and Geodetic latitude.
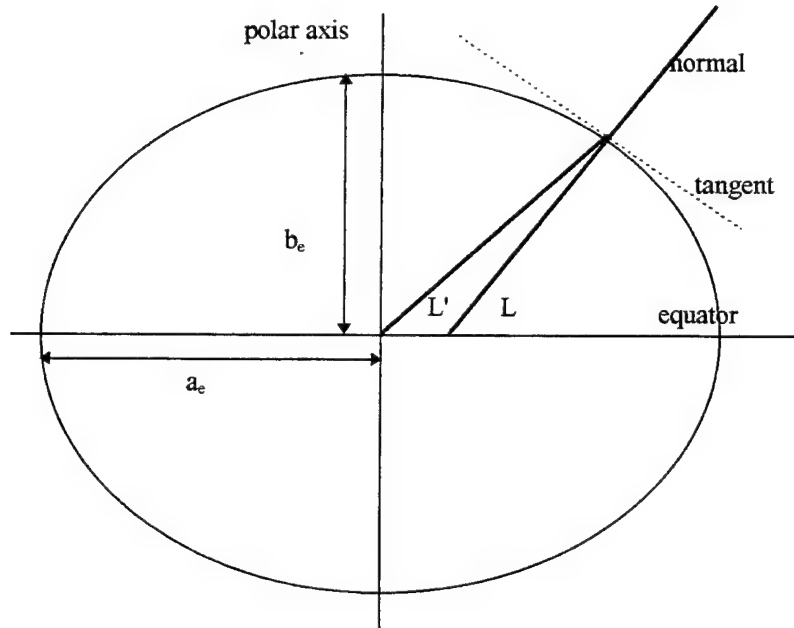
a_e = Equatorial radius (6378.167 Km)
b_e = Polar radius (6356.785 Km)

Figure 13 Geocentric and geodetic latitude

The angle L' is called "geocentric latitude" and is defined as the angle between the equatorial plan and the radius from the geocenter. The angle L is called " geodetic latitude" and is defined as angle between the equatorial plan and the normal to the surface of the ellipsoid. The word "latitude" usually means geodetic latitude.

What we need now is a method of calculating the station coordinates of a point on the surface of our reference ellipsoid when we know the geodetic latitude and longitude of the point and its height above mean sea level. Consider an ellipse comprising and rectangular coordinate system as shown in Figure 14 .
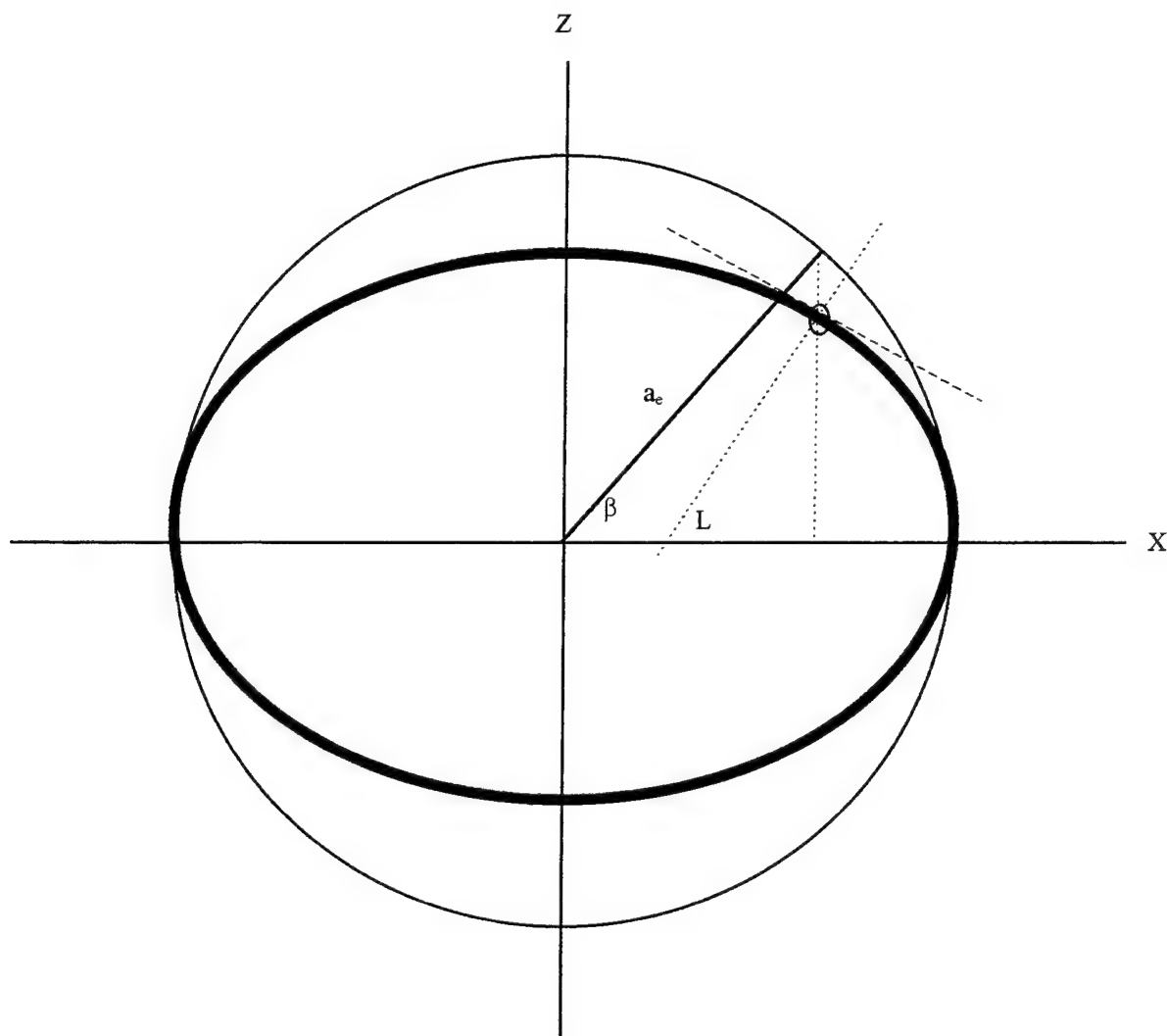
Figure 14 Station Coordinates

We will first determine the X and Z coordinates of a point on the ellipse assuming that we know the geodetic latitude L. It will then be a simple matter to adjust these coordinates for a point which is a known elevation angle above the surface of the ellipsoid in the direction of the normal. It is convenient to introduce the angle β, the "reduced latitude" which is illustrated in Figure 14 . The X and Z coordinates can immediately be written in term of β if we note that the ratio of the z coordinate of the point on the ellipse to the corresponding Z ordinate of a point on the circumscribed circle is just b_e/a_e. Thus,

$$x = a_e \cos \beta$$

$$z = \frac{b_e}{a_e} \, a_e \sin \beta$$

But, for any ellipse , $a^2 = b^2 + c^2$ and $e = c/a$, where e is eccentricity, so

$$b_e = a_e \, \sqrt{1-e^2}$$

and

$$z = a_e \, \sqrt{1-e^2} \, \sin \beta$$

We must now express $\sin \beta$ in terms of the geodetic latitude L and the constants a_e and b_e. From elementary calculus we know that the slope of the tangent to the ellipse is just dz/dx and the slope of the normal is $-dx/dz$. Since the slope of the normal is just $\tan L$, we can write

$$\tan L = - \frac{dx}{dz}$$

The differentials dx and dz can be obtained by differentiating the expressions for x and z above. Thus,

$$dx = - a_e \sin \beta \, d\beta$$

$$dz = a_e \, \sqrt{1-e^2} \, \cos \beta \, d\beta$$

and

$$\tan L = \frac{\tan \beta}{\sqrt{1-e^2}}$$

or

$$\tan \beta = \sqrt{1-e^2} \, \tan L = \frac{\sqrt{1-e^2} \, \sin L}{\cos L}$$

Suppose we consider this last expression as the quotient

$$\tan \beta = \frac{A}{B}$$

where $A = \sqrt{1-e^2} \, \sin L$ and $B = \cos L$.

$$\sin \beta = \frac{\sqrt{1-e^2} \, \sin L}{\sqrt{1-e^2 \, \sin^2 L}}$$

$$\cos \beta = \frac{\cos L}{\sqrt{1-e^2 \, \sin^2 L}}$$

We can now write the x and z coordinates for a point on the ellipse.

$$x = \frac{a_e \, \cos L}{\sqrt{1-e^2 \, \sin^2 L}}$$

$$z = \frac{a_e \, (1 - e^2) \, \sin L}{\sqrt{1-e^2 \, \sin^2 L}}$$

Appendix B

Interface syntax for each subroutine

Subroutine: DIRECT_ACCESS

Calling Syntax:

CALL DIRECT_ACCESS(TDATE, SOURCE, OSTYPE, GRID, DATE,
LFCtropo1, LFCtropo2, PARM, REFHT, UNDUL)

Description of Arguments

Arguments passed from getwxfil subroutine called in Main:

TDATE   : [character*70]
SOURCE   : Data source(ecm,mrf,hiras,user) [integer*2]
OSTYPE   : System type (sun/vax) [character*3]
GRID   : Grid number [integer*4]
DATE   : Date(4) month,hour,day,year in an array [integer*2]
LFCtropo1   : Logical File Code 1 [integer*2]
LFCtropo2   : Logical File Code 2 [integer*2]

Arguments returned to getwxfil subroutine:

PARM   : Parm(1:6), parameter containing information relative
                        to the grid i.e. pressure, temperature, etc [real*8]
REFHT   : Reference height [real*8]
UNDUL   : undulation [real*8]

Subroutine: GEODETIC

Calling Syntax:

    CALL GEODETIC(XLAT, XLON, XH, XX, YY, ZZ, RR)

Descriiption of Arguments

    Arguments passed from position subroutine called in Main:

XLAT	: Geodetic latitude in degree [real*8]
XLON	: Geodetic longitude in degree [real*8]
XH	: Height above reference ellpisoid in kilometer [real*8]

    Arguments returned to position subroutine:

XX	: X ECF coordinate in kilometers [real*8]
YY	: Y ECF coordinate in kilometers [real*8]
ZZ	: Z ECF coordinate in kilometers [real*8]
RR	: Radial distance from earth center to (x,y,z) position in kilometer [real*8]

Subroutine: GRABGRID

Calling Syntax:

CALL GRABGRID(TDATE, DATE, AZ, LFCtropo1, LFCtropo2,
MslFlg, LAT, LON, SOURCE,OSTYPE, PRESS, TEMP, RELHUM,
DATARAY, DATARAYFLG)

Descriiption of Arguments

Arguments passed from getwxfil subroutine called in Main:

TDATE	: [character*70]
DATE	: Date(4) month,hour,day,year in an array [integer*2]
AZ	: Azimuth angle(0-360) [real*8]
LFCtropo1	: Logical File Code 1 [integer*2]
LFCtropo2	: Logical File Code 2 [integer*2]
MslFlg	: Reference (ellipsoid/mean sea level) [integer*2]
LAT	: Latitude in degree [real*8]
LON	: Longitude in degree [real*8]
SOURCE	: Data source(ecm,mrf,hiras,user) [integer*2]
OSTYPE	: System type (sun/vax) [character*3]
PRESSURE	: Surface pressure in millibar [real*8]
TEMP	: Surface temperature in Kelvin [real*8]
RELHUM	: Surface relative humidity [real*8]

Arguments returned to getwxfil subroutine:

DATARAY	: Dataray(0:730,1:8), an array [real*8]
	Contains following: grid number, latitude, longitude, refractivity, height coefficient, range error variance, angle error variance
DATARAYFLG	: Error flag 0--No error during data retrieval 1--error during data retieval

Subroutine: NEWWGS84LATLON

Calling Syntax:

CALL NEWWGS84LATLON(XECF, NEWLAT, NEWLON, ALT, RMAG)

Descriiption of Arguments

Arguments passed from position subroutine called in Main:

XECF   : XECT(7), ECF position   [real*8]

Arguments returned to position subroutine:

NEWLAT   : Geodetic subsatellite latitude in degree [real*8]
NEWLON   : Geodetic subsatellite longitude in degree [real*8]
ALT   : Altitude above ellopsoid   [real*8]
RMAG   : Distance from center to subsatellite point [real*8]

Subroutine: POSITION

Calling Syntax:

CALL POSITION(gdLAT1, gdLON1, ALT1, AZ1, EL1, RHO1, NEWLAT, NEWLON)

Descriiption of Arguments

Arguments passed from raytrace subroutine called in Main:

gdLAT1	: Input latitude in degree [real*8]
gdLON1	: Input longitude in degree [real*8]
ALT1	: Input altitude in meter [real*8]
AZ1	: Input azimuth in degree [real*8]
EL1	: Input elevation in degree [real*8]
RHO1	: Input ray path in kilometers [real*8]

Arguments returned to raytrace subroutine:

NEWLAT	: New latitude position in degree [real*8]
NEWLON	: New longitude position in degree [real*8]
Errflg	: Error flag

Subroutine: USER_INFO

Calling Syntax:

CALL USER_INFO(DATE, LFCtropo1, MslFlg, LAT,LON, PRESS,
TEMP, RELHUM, OSTYPE, DATARAY, DATARAYFLG)

Description of Arguments

Arguments passed from getwxfil subroutine called in Main:

DATE   : Date(4) month, hour,day, and year in array   [integer*2]
LFCtropo1   : Logical File Code 1   [integer*2]
MslFlg   : Reference (ellipsoid/mean sea level) [integer*2]
LAT   : Latitude in degree   [real*8]
LON   : Longitude in degree   [real*8]
PRESS   : Surface pressure in millibar   [real*8]
TEMP   : Surface temperature in Kelvin [real*8]
RELHUM   : Surface relative humidity in percent [real*8]
OSTYPE   : System type (sun/vax) [character*3]

Arguments returned to getwxfil subroutine:

DATARAY   : Dataray(0:730,1:8), an array [real*8]

                  Contains following:
                    grid number, latitude, longitude, refractivity,
                    height coefficient, range error variance,
                    angle error variance
DATARAYFLG   : Error flag
                   0--No error during data retrieval
                   1--error during data retieval

Appendix C

Flow Charts of Data Processing and Source Code

Data Processing Flow Diagram for Tropospheric Propagation Database

HIRAS

a	b	c

· 8 mm tape for 10 years hourly monthly avg. data

a : Temperature files
b : Pressure files
c : Relative Humidity files

ECMWF

· 8 mm tape for 10 years monthly avg. data
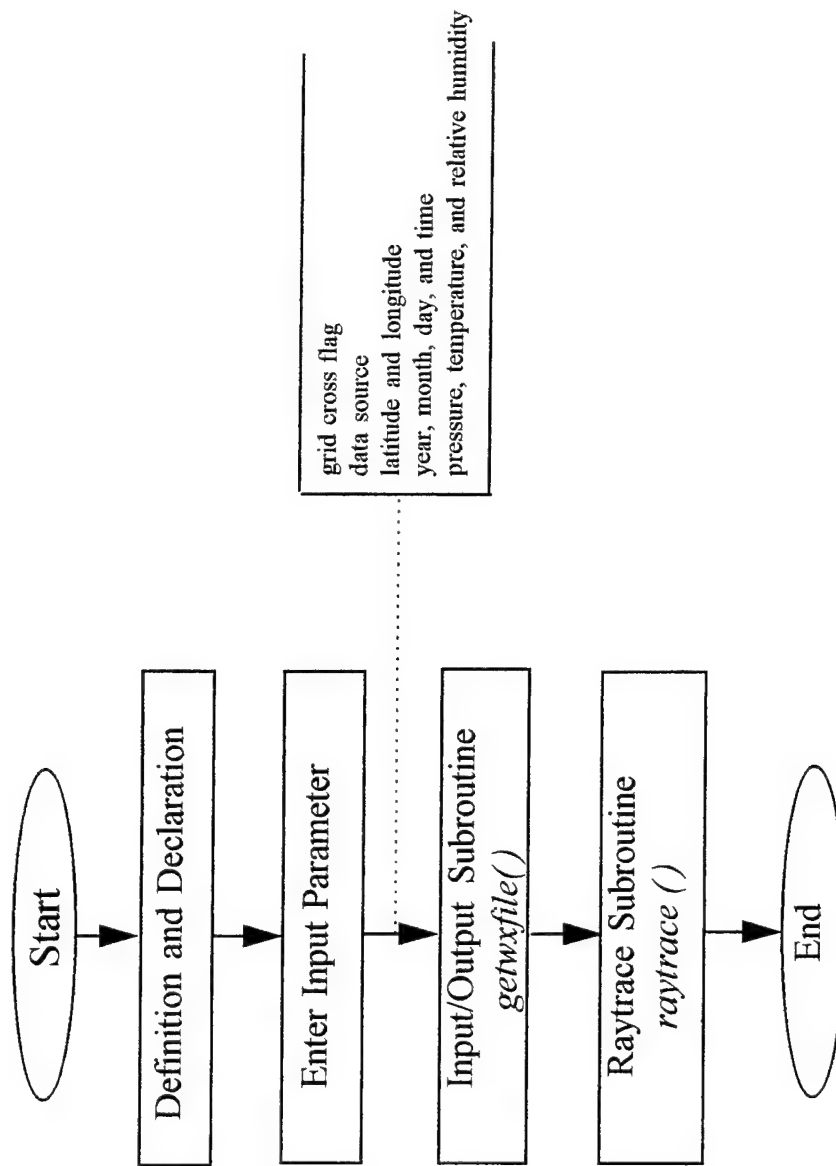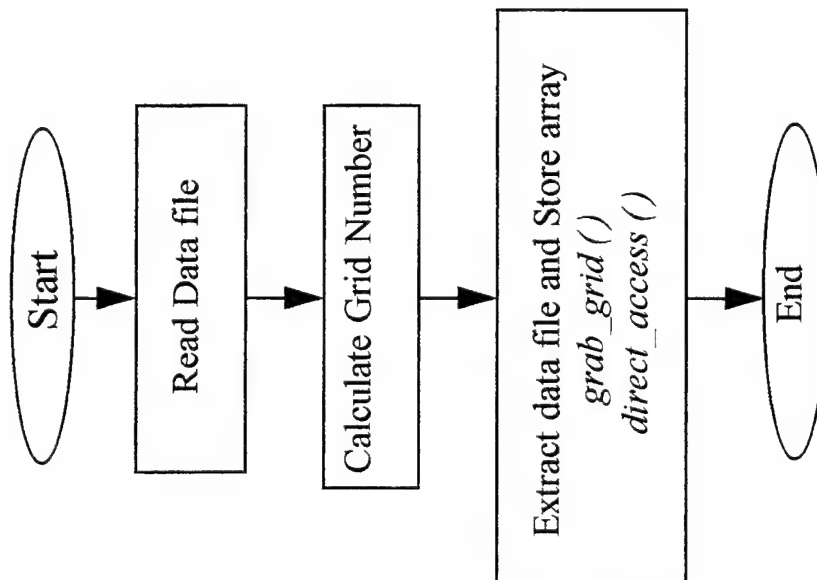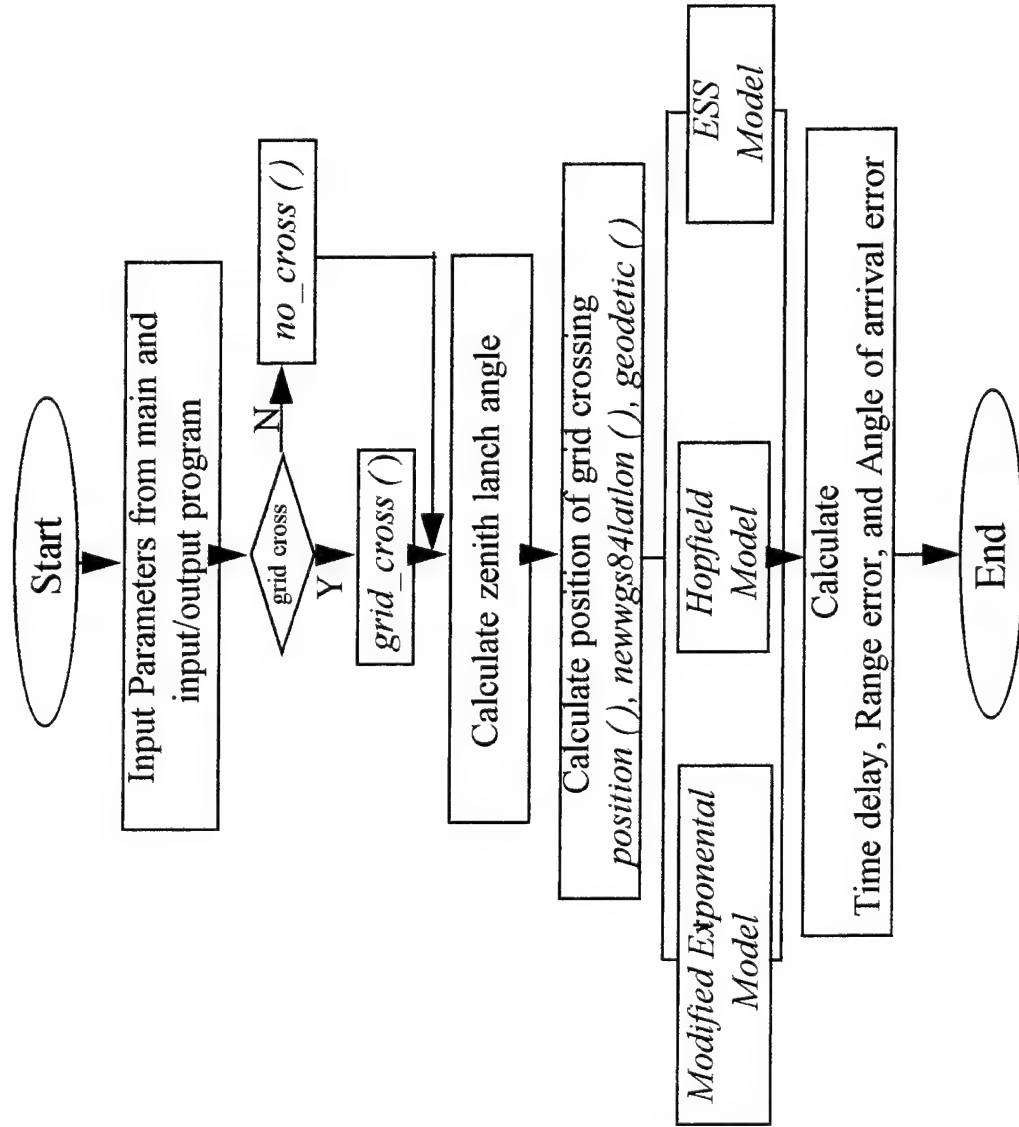
MRF

· Binary data
· 4 time hourly/dairly
· 2.5 x 2.5 degree data
· 1991 - 1996 data

FNL

· Binary data
· 4 time hourly/dairly
· 1.0 x 1.0 degree data
· 1997 - current data

**Real Time
User Input Data**

· Merge a,b, and c data files
· Add ECM height parameter

· Produce Grid-oriented data (2.5 by 2.5)
· Convert dew point to relative humidity
· Convert temperature to Kelvin
· Generate refractivity and statistics; mean & standard deviation for temperature, pressure, and relative humidity
· Calculate hopfield and goad wet/dry high

· Convert ASCII data
· Sort by grid number
· Fill missing data

HIRAS, ECMWF, MRF

· 14 Layers above mean-sea-level by pressure for HIRAS and ECM
12 Layers for MRF 1
· 2.5 X 2.5 degree resolution data
· Month of the year
· Time of the day (0 hr,6 hr,12 hr and 18 hr)

FNL

· 13 Layers above mean-sea-level by pressure level(Mb)
· Month of the year
· Time of the day (0 hr,6 hr,12 hr and 18 hr)
· Add 925 and 20 Mb pressure take off 70 Mb pressure data
· 1.0 X 1.0 degree resolution data

* available 8-mm Magnetic tapes

· Surface information and reference height for hourly dairly monthly yearly data

* available 8-mm Magnetic tapes

51

Flow Chart of Main Program

Start

↓

Definition and Declaration

↓

Enter Input Parameter

↓ ⋯⋯⋯⋯⋯⋯

grid cross flag
data source
latitude and longitude
year, month, day, and time
pressure, temperature, and relative humidity

Input/Output Subroutine
getwxfile( )

↓

Raytrace Subroutine
raytrace ( )

↓

End

52

Flow Chart of Input/Output Program

```
        ┌──────────┐
        │  Start   │
        └────┬─────┘
             │
             ▼
    ┌─────────────────┐
    │  Read Data file  │
    └────────┬─────────┘
             │
             ▼
    ┌─────────────────────┐
    │ Calculate Grid Number │
    └──────────┬──────────┘
               │
               ▼
┌───────────────────────────────┐
│ Extract data file and Store array │
│        grab_grid ( )           │
│        direct_access ( )       │
└───────────────┬───────────────┘
                │
                ▼
        ┌──────────┐
        │   End    │
        └──────────┘
```

Flow Chart of Raytrace Program

Start

Input Parameters from main and input/output program

grid cross

N → no_cross ( )

Y → grid_cross ( )

Calculate zenith lanch angle

Calculate position of grid crossing
position ( ), newwgs84latlon ( ), geodetic ( )

Modified Exponental Model

Hopfield Model

ESS Model

Calculate
Time delay, Range error, and Angle of arrival error

End

Appendix D

Percent Standard Deviations Time Delay

ECMWF Time Delay Percent Standard Deviation Contour Map for Jan (Angle = 0 deg)
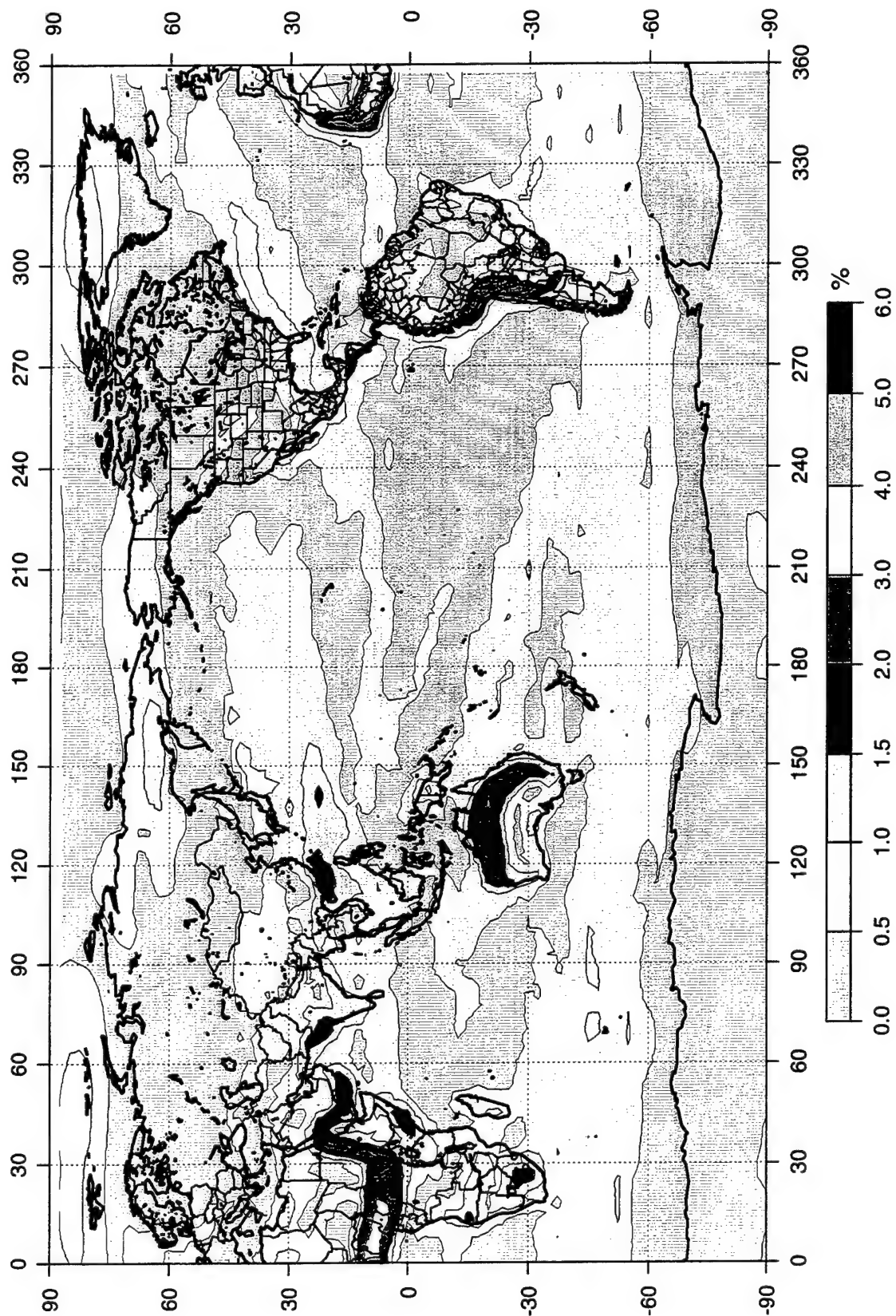
ECMWF Time Delay Percent Standard Deviation Contour Map for Apr (Angle = 0 deg)
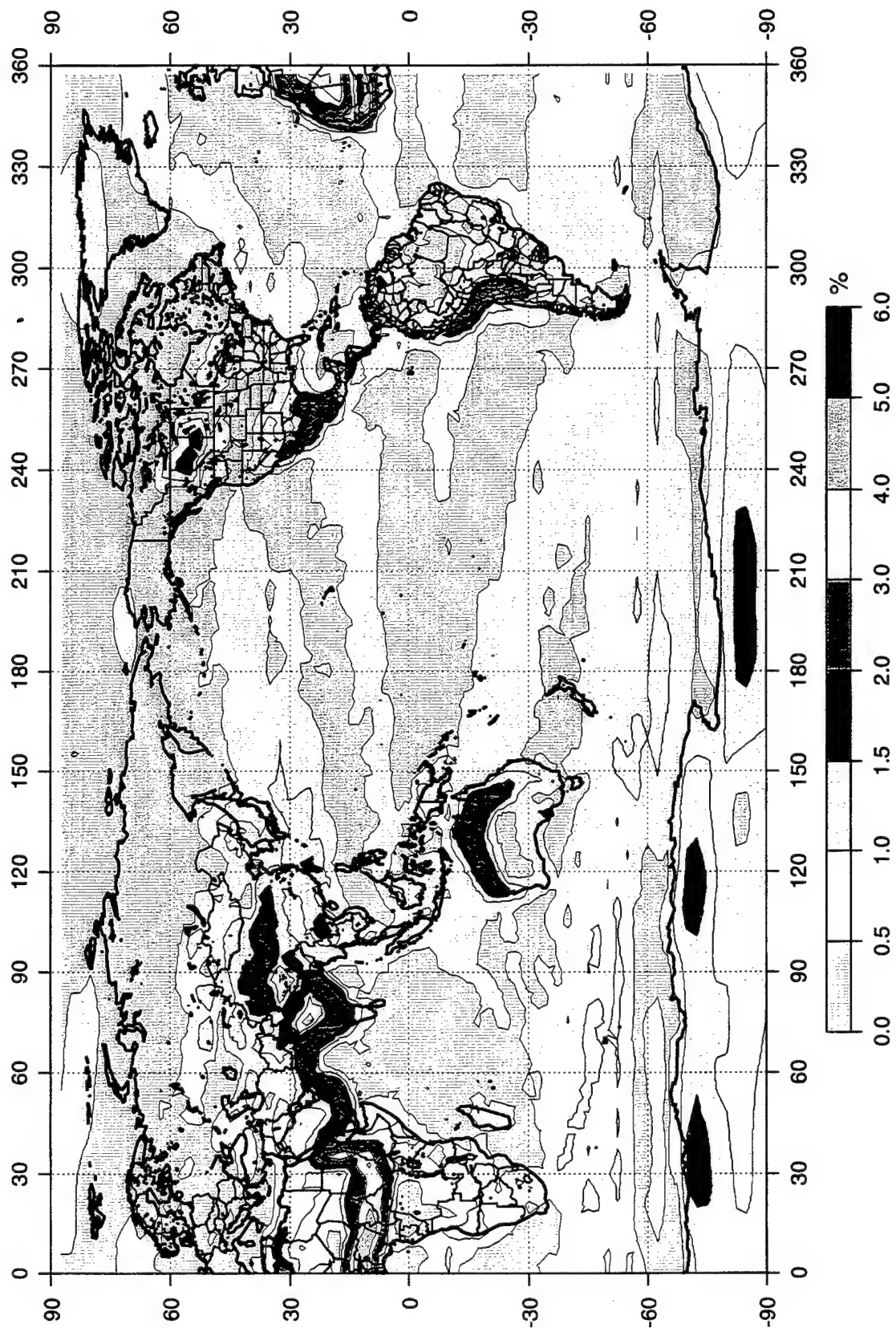
ECMWF Time Delay Percent Standard Deviation Contour Map for Jul (Angle = 0 deg)
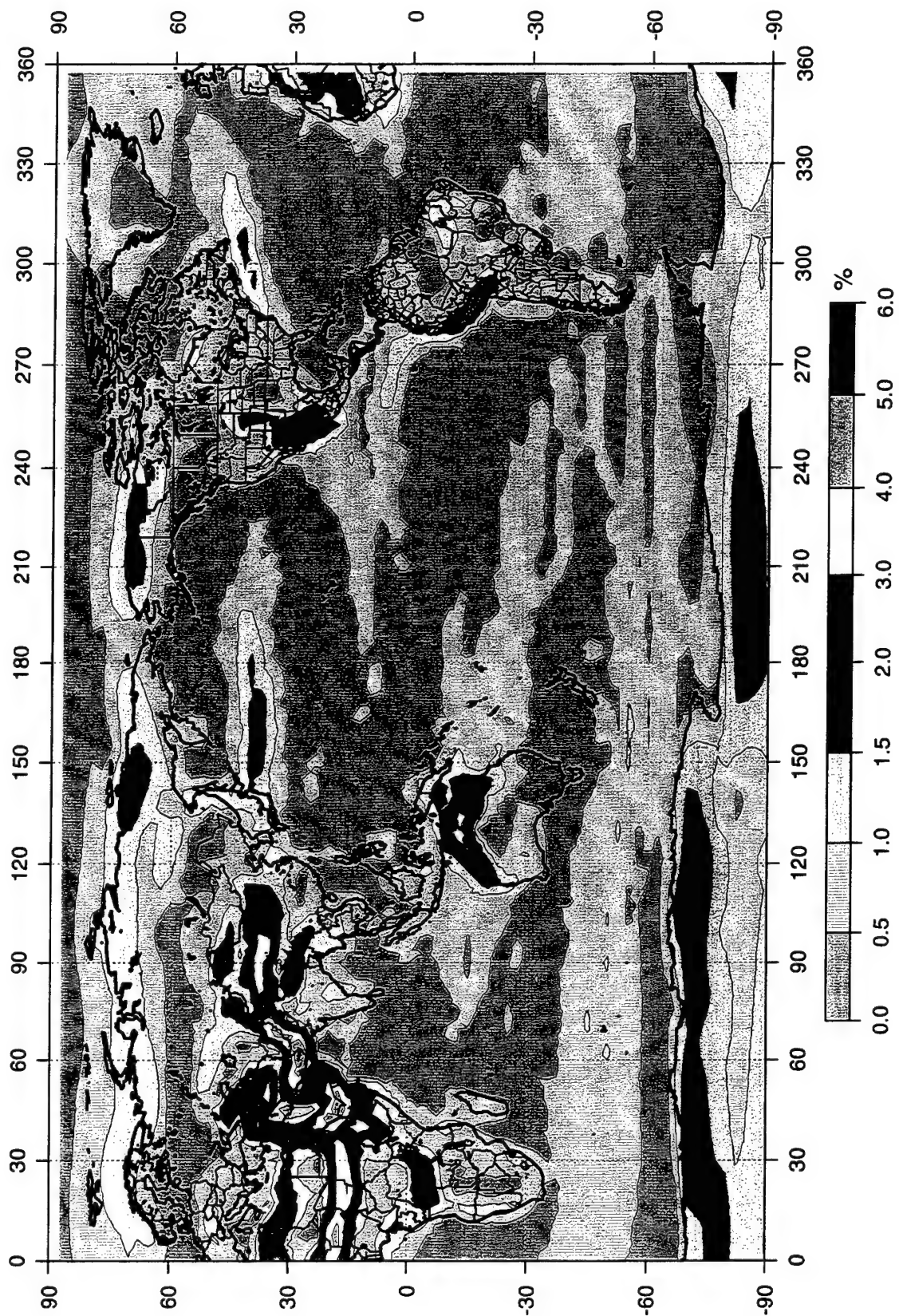
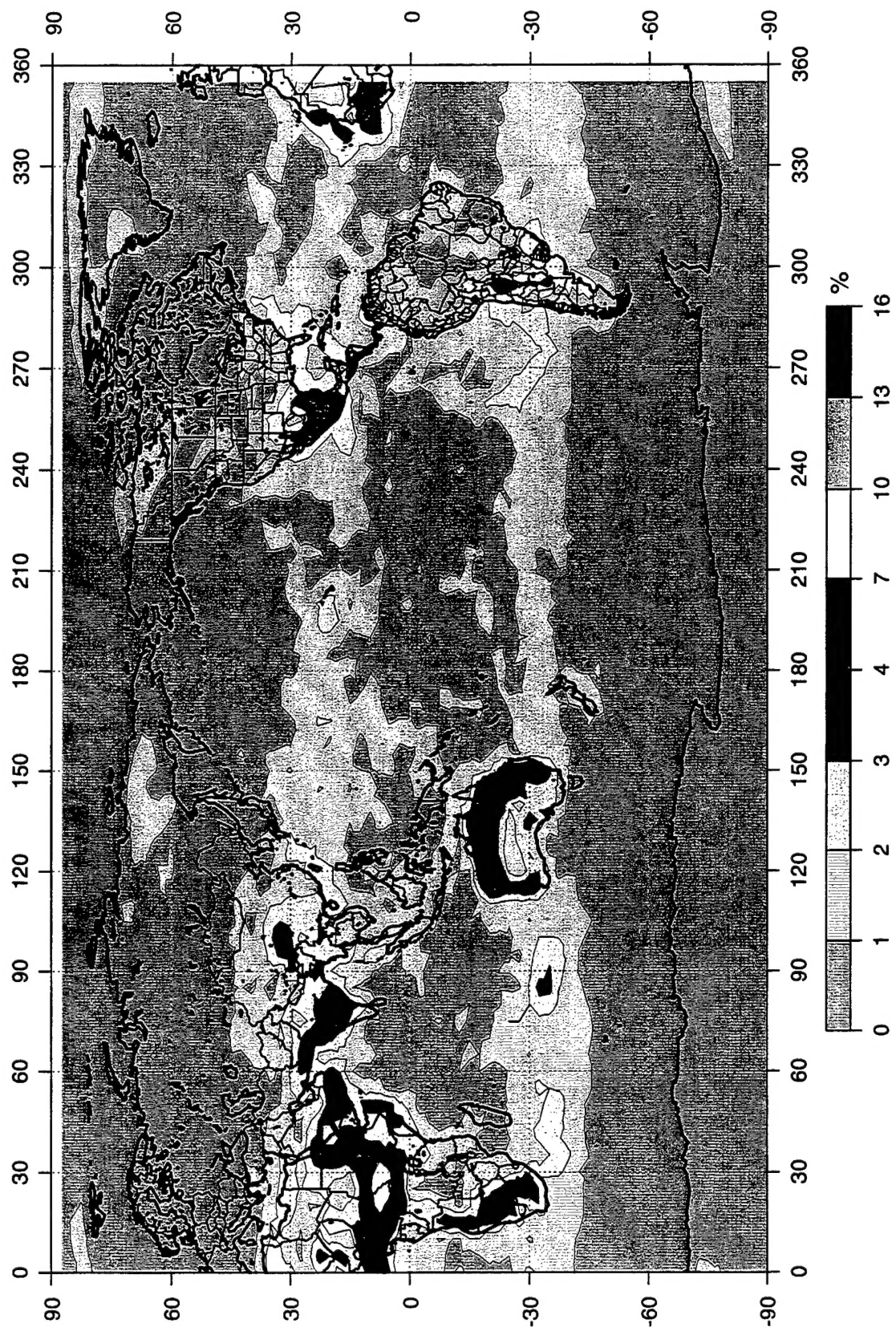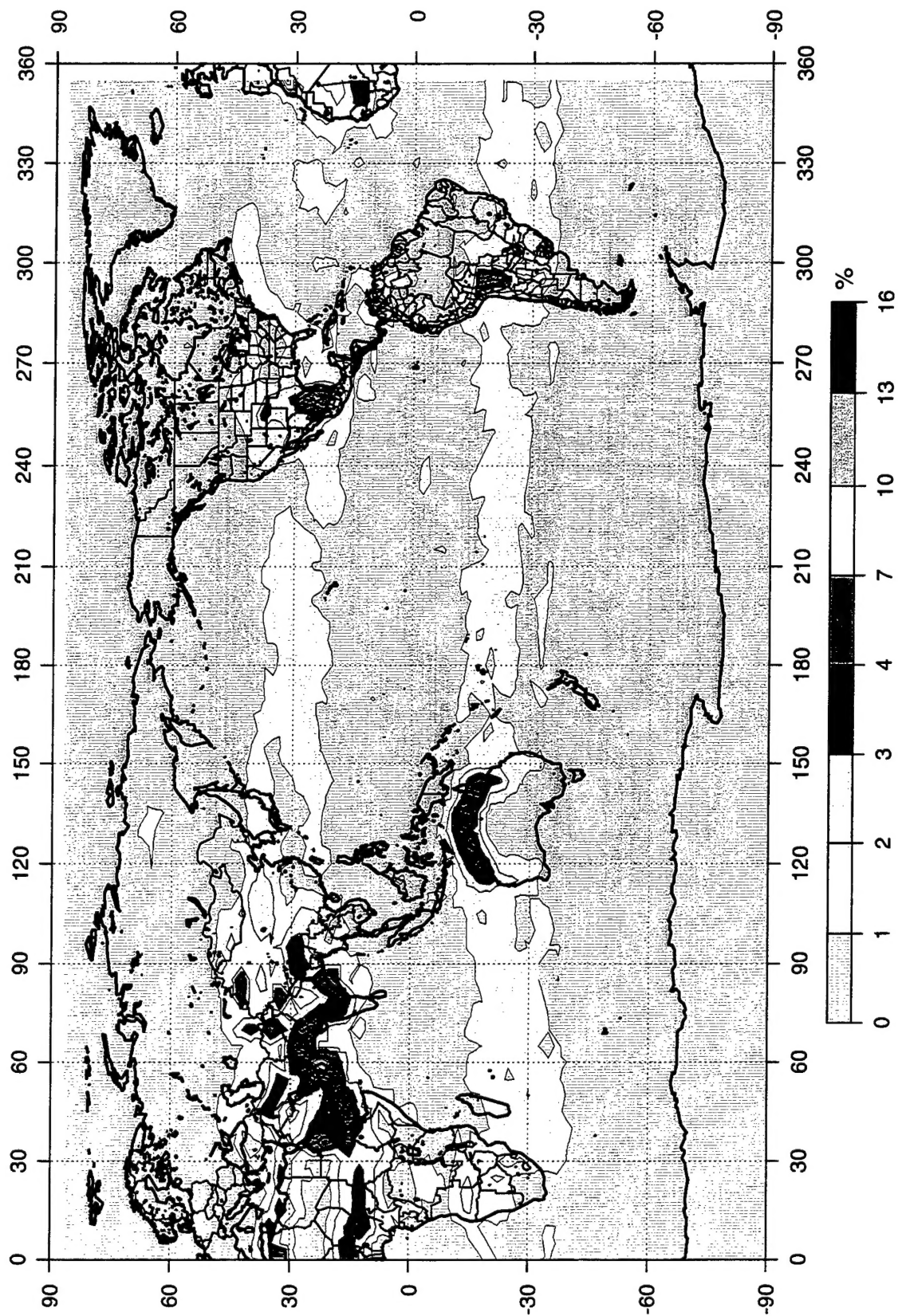ECMWF Time Delay Percent Standard Deviation Contour Map for Oct (Angle = 0 deg)
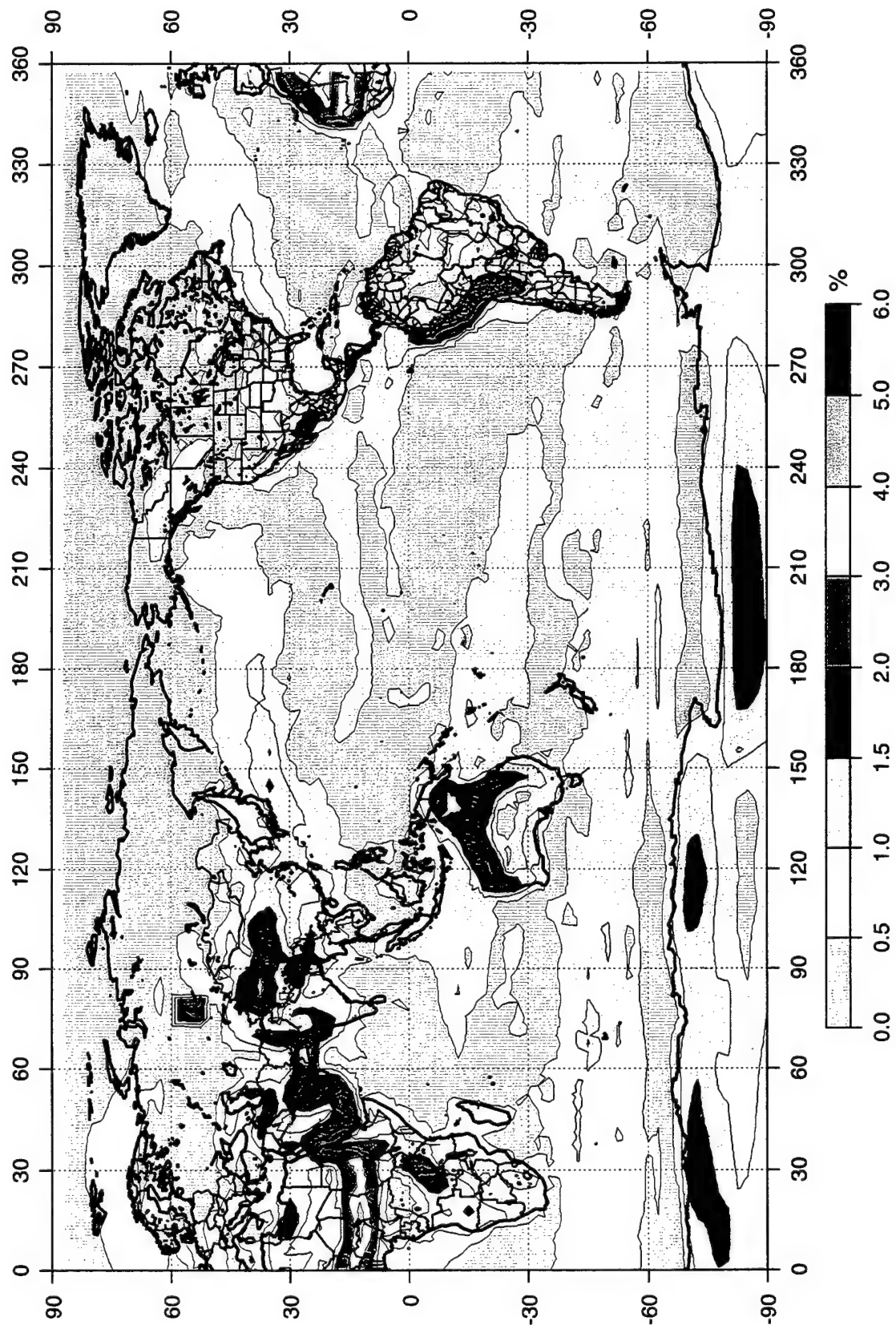
Appendix E
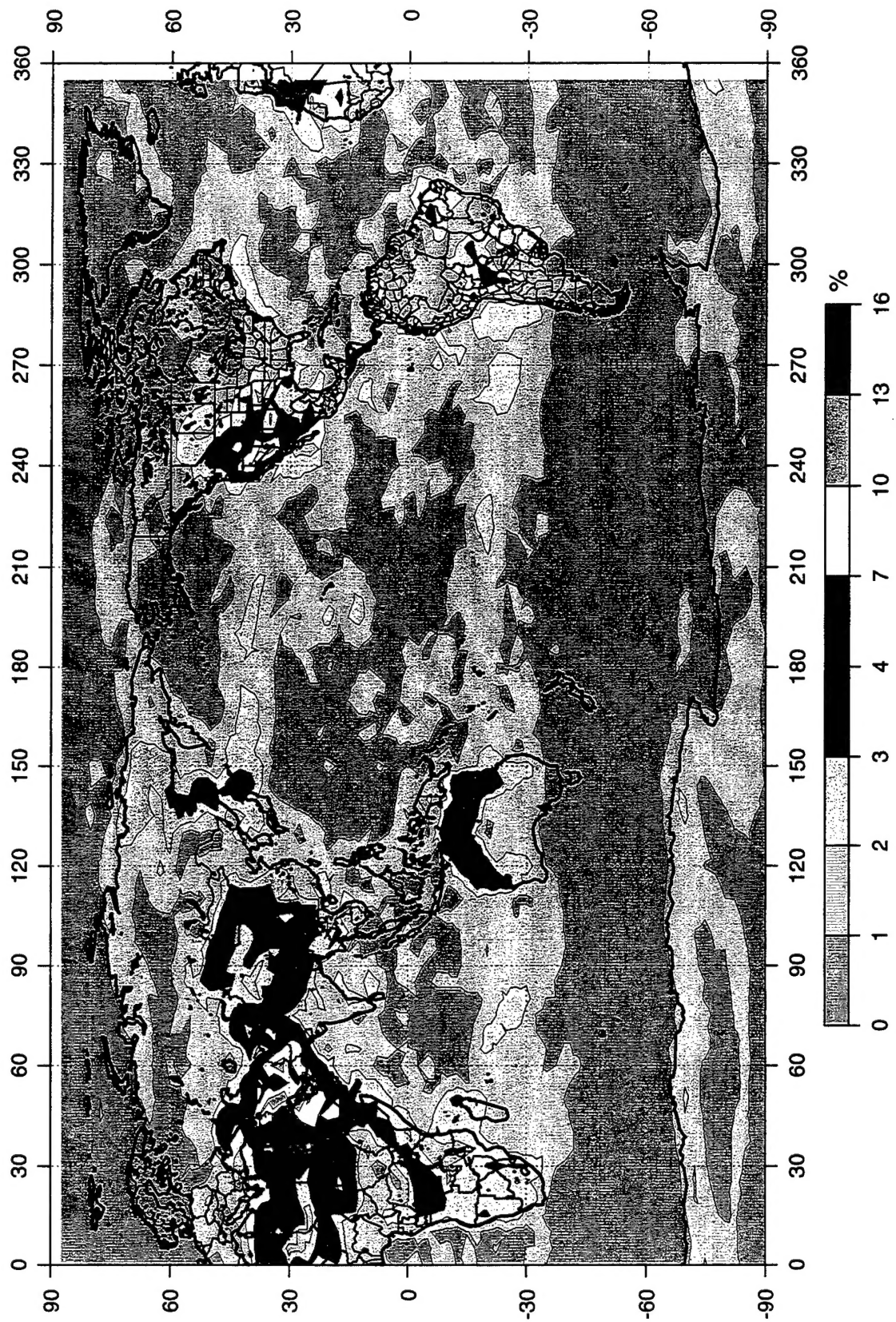
Azimuth Sensitivity HIRAS data

HIRAS Percent Change in Time Delay (Feb 0600 Surface Data, 45 deg Azimuth Increments, Angle = 0 deg)

HIRAS Percent Change in Time Delay (May 0600 Surface Data, 45 deg Azimuth Increments, Angle = 0 deg)

HIRAS Percent Change in Time Delay (Aug 0600 Surface Data, 45 deg Azimuth Increments, Angle = 0 deg)

HiRAS Percent Change in Time Delay (Nov 0600 Surface Data, 45 deg Azimuth Increments, Angle = 0 deg)